0.1 Results: ΛK^0_S and $\Lambda K^{\pm}$

In the following sections, we present results assuming (i) three residual contributors (Sec. 0.1.1), (ii) ten residual contributors (Sec. 0.1.2), and (iii) no residual correlations (Sec. 0.1.3).

For the results shown, unless otherwise noted, the following hold true: All correlation functions were normalized in the range $0.32 < k^* < 0.40$ GeV/c, and fit in the range $0.0 < k^* < 0.30$ GeV/c. For the ΛK^- and $\bar{\Lambda} K^+$ analyses, the region $0.19 < k^* < 0.23$ GeV/c was excluded from the fit to exclude the bump caused by the Ω^- resonance. The non-femtoscopic backgrounds for the ΛK^+ and ΛK^- systems were modeled by a (6^{th}-)order polynomial fit to THERMINATOR simulation, while those for the ΛK^0_S were fit with a simple linear form. The $\Lambda K^+(\bar{\Lambda} K^-)$ radii are shared with $\Lambda K^-(\bar{\Lambda} K^+)$, while the $\Lambda K^0_S(\bar{\Lambda} K^0_S)$ radii are unique. In the figures showing experimental correlation functions with fits, the black solid line represents the primary (ΛK) correlation's contribution to the fit. The green line shows the fit to the non-flat background. The purple points show the fit after all residuals' contributions have been included, and momentum resolution and non-flat background corrections have been applied.

Before beginning, I first collect a summary of my final results in Figure 1. In the summary plot, we show the extracted scattering parameters in the form of a Im[f_0] vs Re[f_0] plot, which includes the d_0 values to the right side. We also show the λ vs. radius parameters for all three of our studied centrality bins. In Fig. 1, three residual contributors were used. For the ΛK^0_S results shown in the figure, the ΛK^0_S and $\bar{\Lambda} K^0_S$ analyses were fit simultaneously across all centralities (0-10%, 10-30%, 30-50%); scattering parameters and a single λ parameter were shared amongst all, the radii were shared amongst results of like-centrality, and each has a unique normalization parameter. For the $\Lambda K^{\pm}$ results shown, all four pair combinations were fit simultaneously (ΛK^+, $\bar{\Lambda} K^-$, ΛK^-, $\bar{\Lambda} K^+$) across all centralities. Scattering parameters were shared between pair-conjugate systems (i.e. a parameter set describing ΛK^+ & $\bar{\Lambda} K^-$, and a separate set describing ΛK^- & $\bar{\Lambda} K^+$). For each centrality, a radius and λ parameters were shared between all pairs. Each analysis has a unique normalization parameter.

0.1.1 3 Residual Correlations Included in Fit

Figure 1 nicely collects and summarizes all of our extracted fit parameters for the case of 3 included residual contributors. Figure 2 presents our extracted fit radii, along with those of other systems previously analyzed by ALICE [**?**], as a function of pair transverse mass (m_{T}). Figures 3, 4, and 5 show the experimental correlation functions with fits, assuming 3 residual contributors, for all studied centralities for $\Lambda\mathrm{K}^0_{\mathrm{S}}$ with $\bar{\Lambda}\mathrm{K}^0_{\mathrm{S}}$, $\Lambda\mathrm{K}^+$ with $\bar{\Lambda}\mathrm{K}^-$, and $\Lambda\mathrm{K}^-$ with $\bar{\Lambda}\mathrm{K}^+$, respectively. The parameter sets extracted from the fits can be found in Tables 5 and 6.

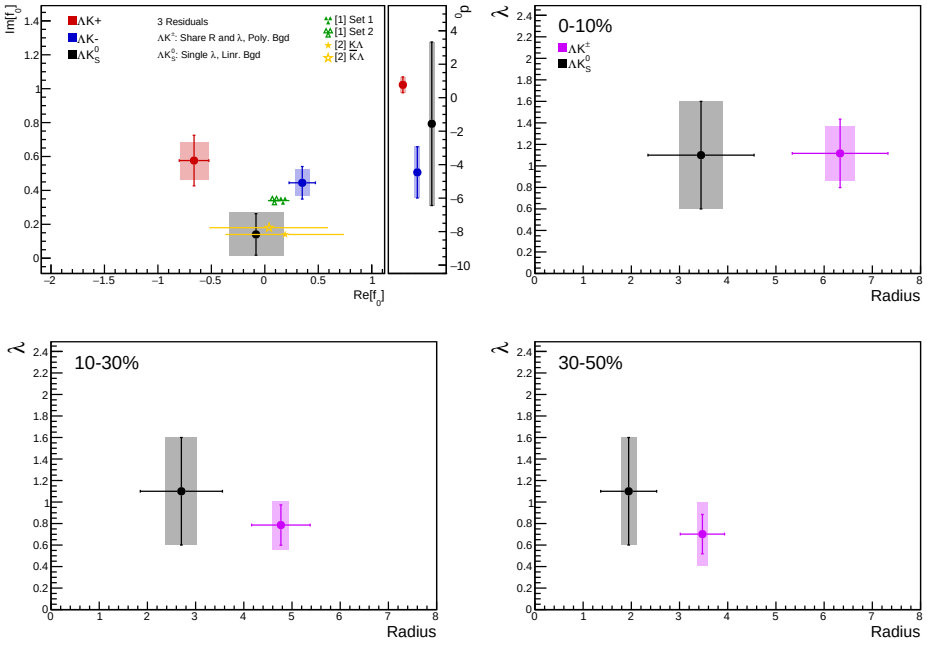

Fig. 1: Extracted scattering parameters for the case of 3 residual contributors for all of our ΛK systems. [Top Left]: $\mathbb{I}f_0$ vs. $\mathbb{R}f_0$, together with d_0 to the right. [Top Right (Bottom Left, Bottom Right)]: λ vs. Radius for the 0-10% (10-30%, 30-50%) bin. The green [**?**] and yellow [**?**] points show theoretical predictions made using chiral perturbation theory.

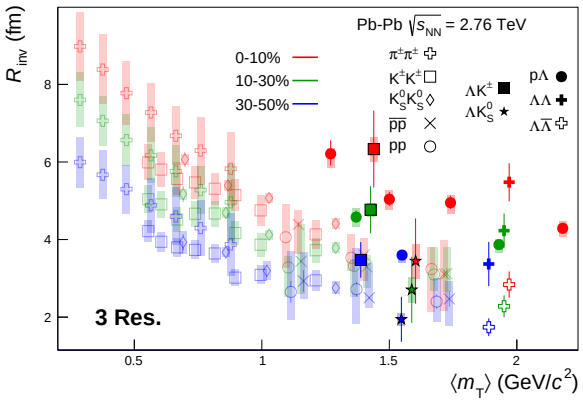

Fig. 2: 3 residual correlations in ΛK fits. Extracted fit R_{inv} parameters as a function of pair transverse mass (m_{T}) for various pair systems over several centralities. The ALICE published data [**?**] is shown with transparent, open symbols. The new ΛK results are shown with opaque, filled symbols. In the left, the $\Lambda\mathrm{K}^+$ (with it's conjugate pair) results are shown separately from the $\Lambda\mathrm{K}^-$ (with it's conjugate pair) results. In the right, all $\Lambda\mathrm{K}^{\pm}$ results are averaged.

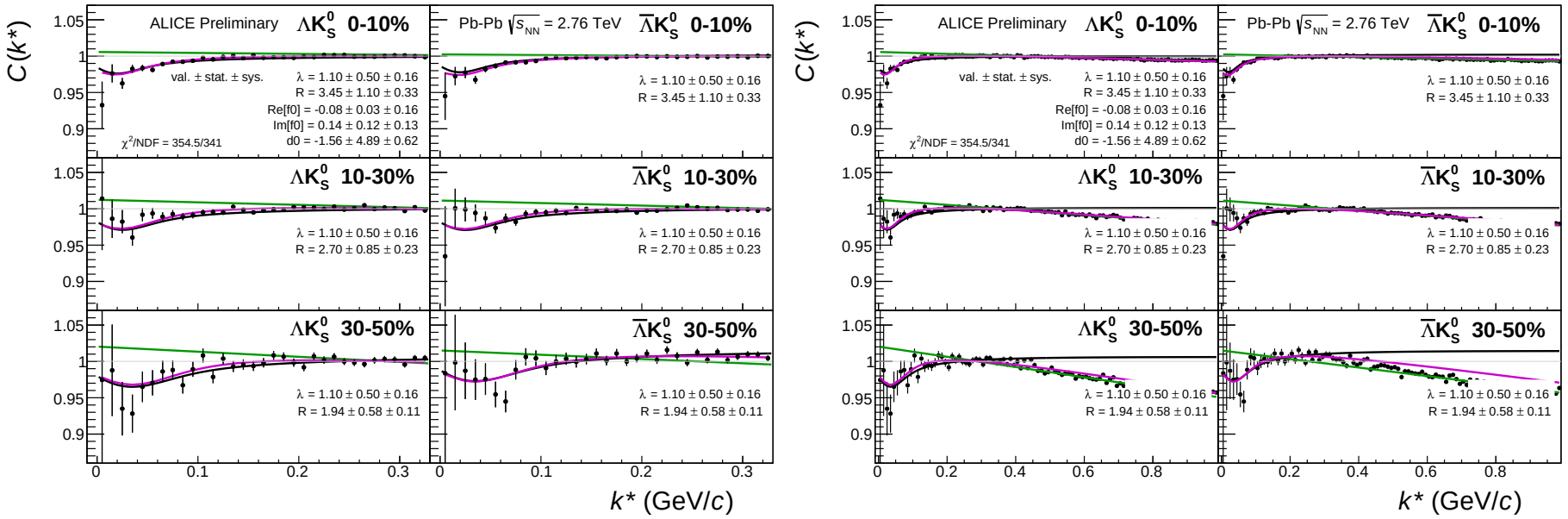

(a) Signal region view ($k^* \lesssim 0.3$ GeV/c)

(b) Wide view ($k^* \lesssim 1.0$ GeV/c)

Fig. 3: Fits, with 3 residual correlations included, to the ΛK^0_S (left) and $\bar{\Lambda} K^0_S$ (right) data for the centralities 0-10% (top), 10-30% (middle), and 30-50% (bottom). The lines represent the statistical errors, while the boxes represent the systematic errors. A single λ parameter is shared amongst all. Each analysis has a unique normalization parameter. The radii are shared between analyses of like centrality, as these should have similar source sizes. The scattering parameters ($\mathbb{R}f_0$, $\mathbb{I}f_0$, d_0) are shared amongst all. The background is modeled by a (6^{th}-)degree polynomial fit to THERMINATOR simulation. The black solid line represents the primary (ΛK) correlation's contribution to the fit. The green line shows the fit to the non-flat background. The purple points show the fit after all residuals' contributions have been included, and momentum resolution and non-flat background corrections have been applied. The extracted fit values with uncertainties are printed.

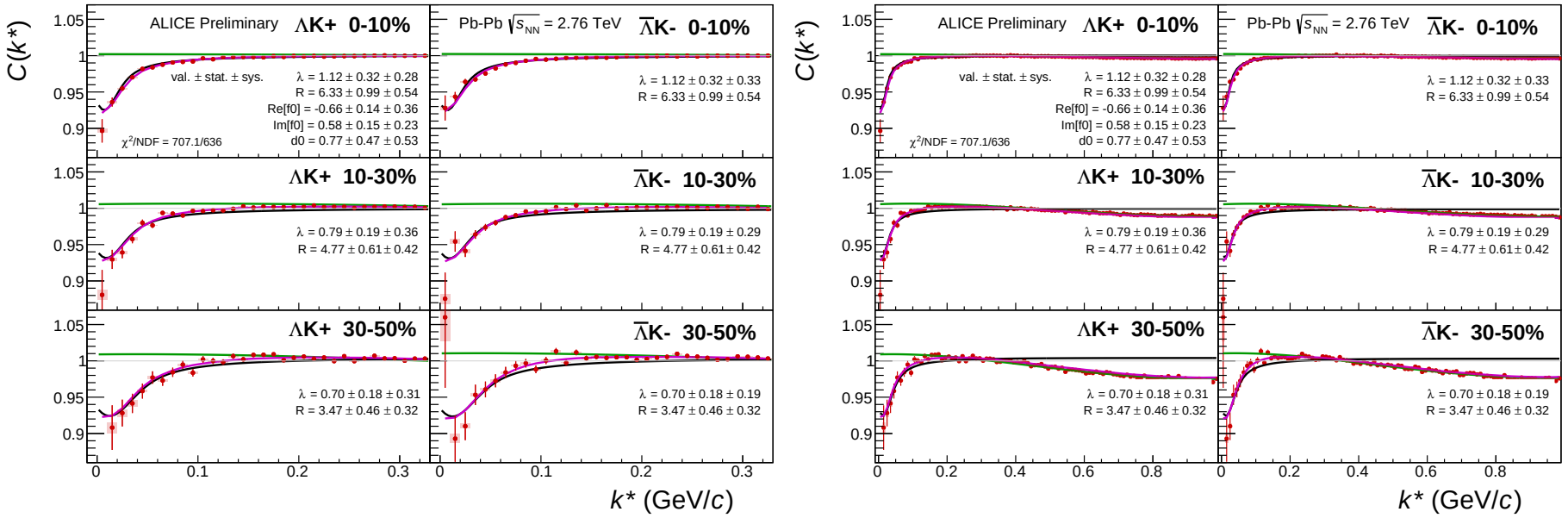

(a) Signal region view ($k^* \lesssim 0.3$ GeV/c)

(b) Wide view ($k^* \lesssim 1.0$ GeV/c)

Fig. 4: Fits, with 3 residual correlations included, to the ΛK^+ (left) and $\bar{\Lambda}K^-$ (right) data for the centralities 0-10% (top), 10-30% (middle), and 30-50% (bottom). The lines represent the statistical errors, while the boxes represent the systematic errors. All $\Lambda K^{\pm}$ analyses are fit simultaneously across all centralities (0-10%, 10-30%, 30-50%). Scattering parameters ($\mathbb{R}f_0$, $\mathbb{I}f_0$, d_0) are shared between pair-conjugate systems (i.e. a parameter set describing the ΛK^+ & $\bar{\Lambda}K^-$ system, and a separate set describing the ΛK^- & $\bar{\Lambda}K^+$ system). For each centrality, a radius and λ parameters are shared between all pairs (ΛK^+, $\bar{\Lambda}K^-$, ΛK^-, $\bar{\Lambda}K^+$). Each analysis has a unique normalization parameter. The background is modeled by a (6^{th}-)degree polynomial fit to THERMINATOR simulation. The black solid line represents the primary (ΛK) correlation's contribution to the fit. The green line shows the fit to the non-flat background. The purple points show the fit after all residuals' contributions have been included, and momentum resolution and non-flat background corrections have been applied. The extracted fit values with uncertainties are printed.

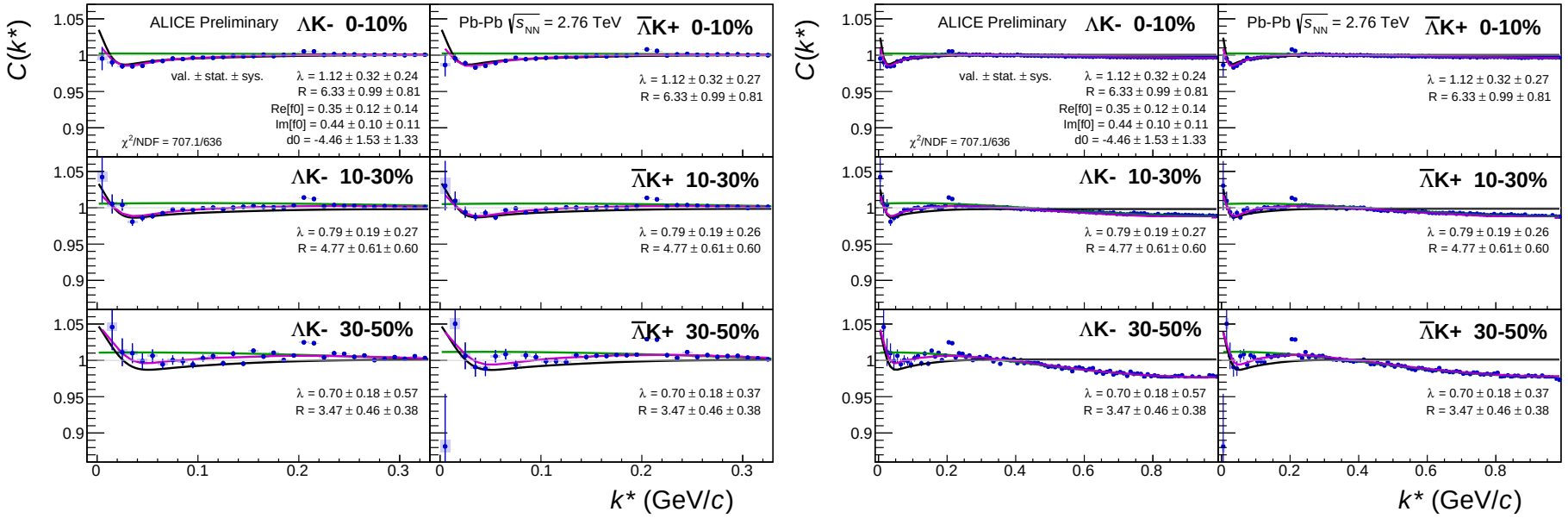

(a) Signal region view ($k^* \lesssim 0.3$ GeV/c)

(b) Wide view ($k^* \lesssim 1.0$ GeV/c)

Fig. 5: Fits, with 3 residual correlations included, to the ΛK^- (left) with $\bar{\Lambda}K^+$ (right) data for the centralities 0-10% (top), 10-30% (middle), and 30-50% (bottom). The lines represent the statistical errors, while the boxes represent the systematic errors. All $\Lambda K^{\pm}$ analyses are fit simultaneously across all centralities (0-10%, 10-30%, 30-50%). Scattering parameters ($\mathbb{R}f_0$, $\mathbb{I}f_0$, d_0) are shared between pair-conjugate systems (i.e. a parameter set describing the ΛK^+ & $\bar{\Lambda}K^-$ system, and a separate set describing the ΛK^- & $\bar{\Lambda}K^+$ system). For each centrality, a radius and λ parameters are shared between all pairs (ΛK^+, $\bar{\Lambda}K^-$, ΛK^-, $\bar{\Lambda}K^+$). Each analysis has a unique normalization parameter. The background is modeled by a (6^{th}-)degree polynomial fit to THERMINATOR simulation. The black solid line represents the "raw" fit, i.e. not corrected for momentum resolution effects nor non-flat background. The green line shows the fit to the non-flat background. The purple points show the fit after momentum resolution and non-flat background corrections have been applied. The extracted fit values with uncertainties are printed.

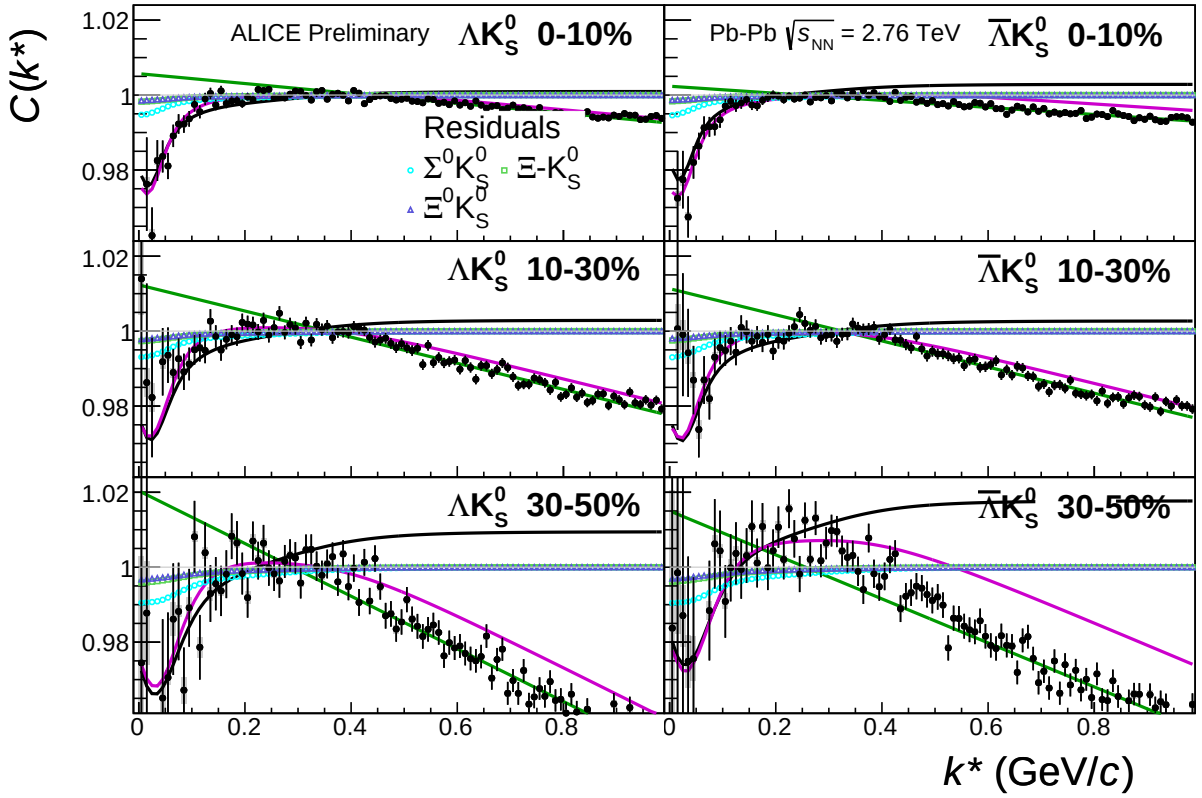

Fig. 6: Fits, with 3 residual correlations included and shown, to the ΛK^0_S (left) and $\bar{\Lambda} K^0_S$ (right) data for the centralities 0-10% (top), 10-30% (middle), and 30-50% (bottom). The three parent pairs used for the residual correction to the ΛK^0_S ($\bar{\Lambda} K^0_S$) fit are $\Sigma^0 K^0_S$, $\Xi^0 K^0_S$, and $\Xi^- K^0_S$ ($\bar{\Sigma}^0 K^0_S$, $\bar{\Xi}^0 K^0_S$, and $\bar{\Xi}^+ K^0_S$).

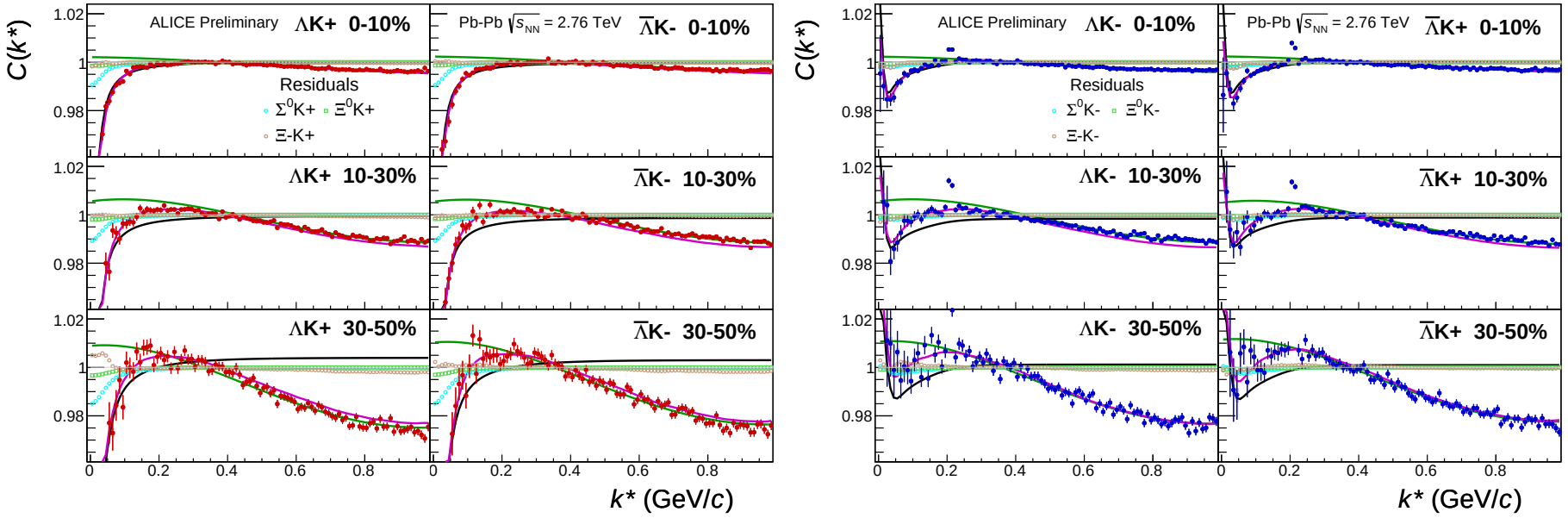

(a) $\Lambda K^+(\bar{\Lambda}K^-)$ fits with residual contributions shown for the centralities 0-10% (top), 10-30% (middle), and 30-50% (bottom)

(b) $\Lambda K^-(\bar{\Lambda}K^+)$ fits with residual contributions shown for the centralities 0-10% (top), 10-30% (middle), and 30-50% (bottom)

Fig. 7: Fits, with 3 residual correlations included and shown, to the ΛK^+ & $\bar{\Lambda}K^-$ (left) and ΛK^- & $\bar{\Lambda}K^+$ (right) data for the centralities 0-10% (top), 10-30% (middle), and 30-50% (bottom). The three parent pairs used for the residual correction to the ΛK^+ ($\bar{\Lambda}K^-$) fit are Σ^0K^+, Ξ^0K^+, and Ξ^-K^+ ($\bar{\Sigma}^0K^-$, $\bar{\Xi}^0K^-$, and $\bar{\Xi}^+K^-$).

Fit Results $\Lambda(\bar{\Lambda})K^0_S$

System	Centrality	Fit Parameters				
		λ	R	$\mathbb{R}f_0$	$\mathbb{I}f_0$	d_0
ΛK^0_S & $\bar{\Lambda}K^0_S$	0-10%	1.10 ± 0.50 (stat.) ± 0.50 (sys.)	3.45 ± 1.10 (stat.) ± 0.45 (sys.)	-0.08 ± 0.03 (stat.) ± 0.25 (sys.)	0.14 ± 0.12 (stat.) ± 0.13 (sys.)	-1.56 ± 4.89 (stat.) ± 3.53 (sys.)
	10-30%		2.70 ± 0.85 (stat.) ± 0.32 (sys.)			
	30-50%		1.94 ± 0.58 (stat.) ± 0.16 (sys.)			

Table 1: Fit Results $\Lambda(\bar{\Lambda})K^0_S$, with 3 residual correlations included. Each pair is fit simultaneously with its conjugate (ie. ΛK^0_S with $\bar{\Lambda}K^0_S$) across all centralities (0-10%, 10-30%, 30-50%), for a total of 6 simultaneous analyses in the fit. A single λ parameter is shared amongst all. Each analysis has a unique normalization parameter. The radii are shared between analyses of like centrality, as these should have similar source sizes. The scattering parameters ($\mathbb{R}f_0$, $\mathbb{I}f_0$, d_0) are shared amongst all. The background is fit with a linear form in the range $0.6 < k^* < 0.9$ GeV/c. The fit is done on the data with only statistical error bars. The errors marked as "stat." are those returned by MINUIT. The errors marked as "sys." are those which result from my systematic analysis (as outlined in Section **??**).

Fit Results $\Lambda(\bar{\Lambda})K^{\pm}$

System	Centrality	Fit Parameters				
		λ	R	$\mathbb{R}f_0$	$\mathbb{I}f_0$	d_0
ΛK^+ & $\bar{\Lambda}K^-$	0-10%	1.12 ± 0.32 (stat.) ± 0.25 (sys.)	6.33 ± 0.99 (stat.) ± 0.31 (sys.)	-0.66 ± 0.14 (stat.) ± 0.13 (sys.)	0.58 ± 0.15 (stat.) ± 0.11 (sys.)	0.77 ± 0.47 (stat.) ± 1.66 (sys.)
	10-30%	0.79 ± 0.19 (stat.) ± 0.23 (sys.)	4.77 ± 0.61 (stat.) ± 0.17 (sys.)			
ΛK^+ & $\bar{\Lambda}K^-$	30-50%	0.70 ± 0.18 (stat.) ± 0.30 (sys.)	3.47 ± 0.46 (stat.) ± 0.10 (sys.)	0.35 ± 0.12 (stat.) ± 0.07 (sys.)	0.44 ± 0.10 (stat.) ± 0.08 (sys.)	-4.46 ± 1.53 (stat.) ± 1.36 (sys.)

Table 2: Fit Results $\Lambda(\bar{\Lambda})K^{\pm}$, with 3 residual correlations included. All $\Lambda K^{\pm}$ analyses are fit simultaneously across all centralities (0-10%, 10-30%, 30-50%). Scattering parameters ($\mathbb{R}f_0$, $\mathbb{I}f_0$, d_0) are shared between pair-conjugate systems (i.e. a parameter set describing the ΛK^+ & $\bar{\Lambda}K^-$ system, and a separate set describing the ΛK^- & $\bar{\Lambda}K^+$ system). For each centrality, a radius and λ parameters are shared between all pairs (ΛK^+, $\bar{\Lambda}K^-$, ΛK^-, $\bar{\Lambda}K^+$). Each analysis has a unique normalization parameter. The background is modeled by a (6^{th}-)degree polynomial fit to THERMINATOR simulation. The fit is done on the data with only statistical error bars. The errors marked as "stat." are those returned by MINUIT. The errors marked as "sys." are those which result from my systematic analysis (as outlined in Section **??**).

0.1.2 10 Residual Correlations Included in Fit

Figure 8 nicely collects and summarizes all of our extracted fit parameters for the case of 10 included residual contributors. Figure 9 presents our extracted fit radii, along with those of other systems previously analyzed by ALICE [**?**], as a function of pair transverse mass (m_{T}). Figures 10, 11, and 12 show the experimental correlation functions with fits, assuming 10 residual contributors, for all studied centralities for $\Lambda\mathrm{K}^0_{\mathrm{S}}$ with $\bar{\Lambda}\mathrm{K}^0_{\mathrm{S}}$, $\Lambda\mathrm{K}^+$ with $\bar{\Lambda}\mathrm{K}^-$, and $\Lambda\mathrm{K}^-$ with $\bar{\Lambda}\mathrm{K}^+$, respectively. The parameter sets extracted from the fits can be found in Tables **??** and **??**.

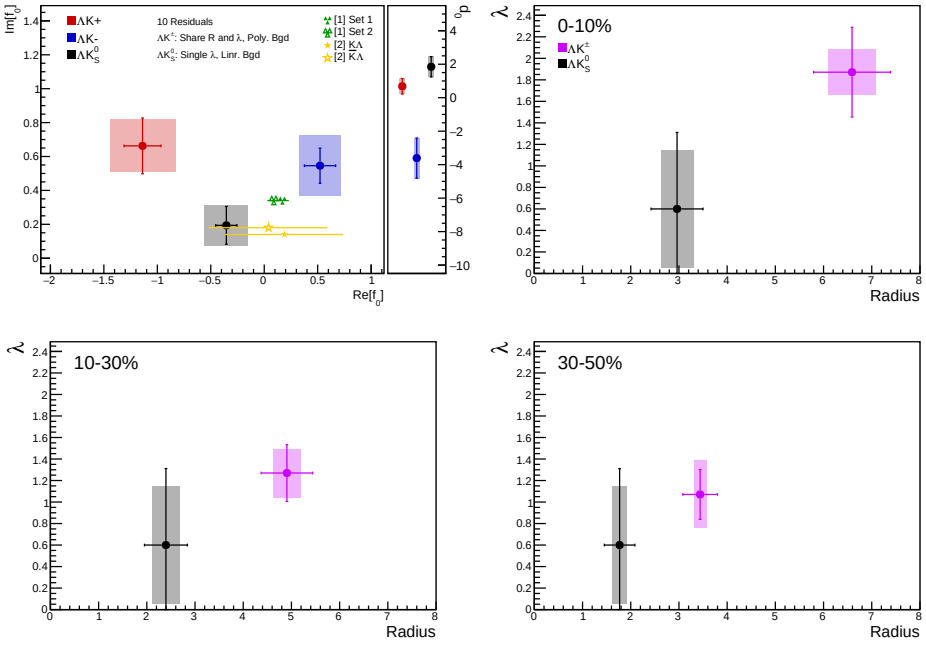

Fig. 8: Extracted scattering parameters for the case of 10 residual contributors for all of our ΛK systems. [Top Left]: $\mathbb{I}f_0$ vs. $\mathbb{R}f_0$, together with d_0 to the right. [Top Right (Bottom Left, Bottom Right)]: λ vs. Radius for the 0-10% (10-30%, 30-50%) bin. The green [**?**] and yellow [**?**] points show theoretical predictions made using chiral perturbation theory.

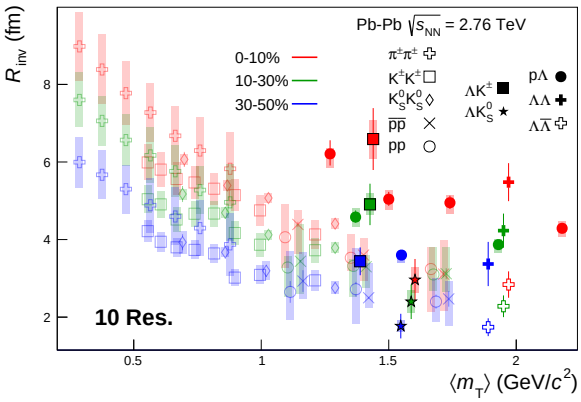

Fig. 9: 10 residual correlations in ΛK fits. Extracted fit R_{inv} parameters as a function of pair transverse mass (m_{T}) for various pair systems over several centralities. The ALICE published data [**?**] is shown with transparent, open symbols. The new ΛK results are shown with opaque, filled symbols. In the left, the $\Lambda\mathrm{K}^+$ (with it's conjugate pair) results are shown separately from the $\Lambda\mathrm{K}^-$ (with it's conjugate pair) results. In the right, all $\Lambda\mathrm{K}^{\pm}$ results are averaged.

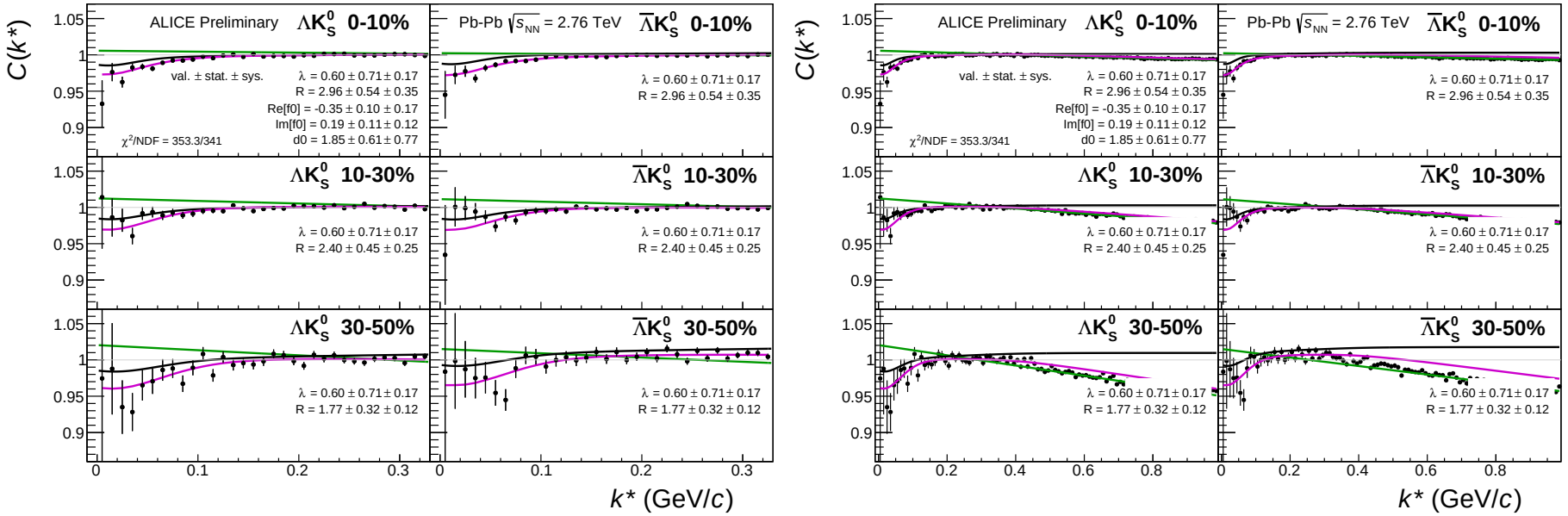

(a) Signal region view ($k^* \lesssim 0.3$ GeV/c)

(b) Wide view ($k^* \lesssim 1.0$ GeV/c)

Fig. 10: Fits, with 10 residual correlations included, to the ΛK^0_S (left) and $\bar{\Lambda} K^0_S$ (right) data for the centralities 0-10% (top), 10-30% (middle), and 30-50% (bottom). The lines represent the statistical errors, while the boxes represent the systematic errors. A single λ parameter is shared amongst all. Each analysis has a unique normalization parameter. The radii are shared between analyses of like centrality, as these should have similar source sizes. The scattering parameters ($\mathbb{R}f_0$, $\mathbb{I}f_0$, d_0) are shared amongst all. The background is modeled by a (6^{th}-)degree polynomial fit to THERMINATOR simulation. The black solid line represents the primary (ΛK) correlation's contribution to the fit. The green line shows the fit to the non-flat background. The purple points show the fit after all residuals' contributions have been included, and momentum resolution and non-flat background corrections have been applied. The extracted fit values with uncertainties are printed.

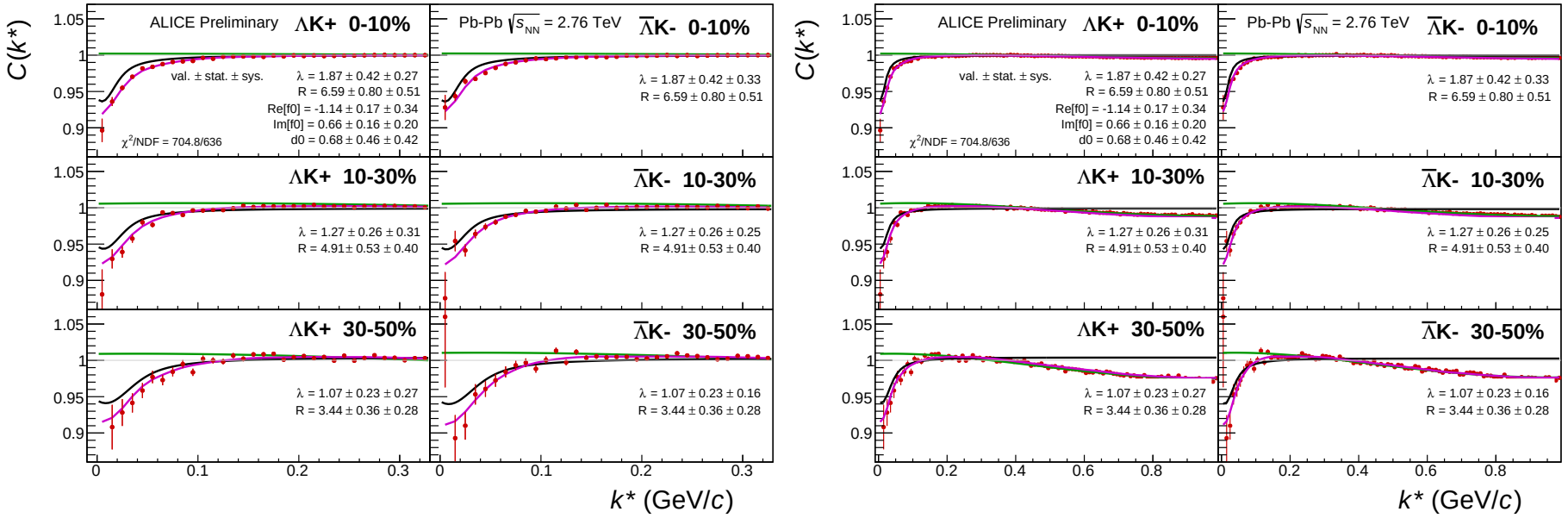

(a) Signal region view ($k^* \lesssim 0.3$ GeV/c)

(b) Wide view ($k^* \lesssim 1.0$ GeV/c)

Fig. 11: Fits, with 10 residual correlations included, to the ΛK^+ (left) and $\bar{\Lambda}K^-$ (right) data for the centralities 0-10% (top), 10-30% (middle), and 30-50% (bottom). The lines represent the statistical errors, while the boxes represent the systematic errors. All $\Lambda K^{\pm}$ analyses are fit simultaneously across all centralities (0-10%, 10-30%, 30-50%). Scattering parameters ($\mathbb{R}f_0$, $\mathbb{I}f_0$, d_0) are shared between pair-conjugate systems (i.e. a parameter set describing the ΛK^+ & $\bar{\Lambda}K^-$ system, and a separate set describing the ΛK^- & $\bar{\Lambda}K^+$ system). For each centrality, a radius and λ parameters are shared between all pairs (ΛK^+, $\bar{\Lambda}K^-$, ΛK^-, $\bar{\Lambda}K^+$). Each analysis has a unique normalization parameter. The background is modeled by a (6^{th}-)degree polynomial fit to THERMINATOR simulation. The black solid line represents the primary (ΛK) correlation's contribution to the fit. The green line shows the fit to the non-flat background. The purple points show the fit after all residuals' contributions have been included, and momentum resolution and non-flat background corrections have been applied. The extracted fit values with uncertainties are printed.

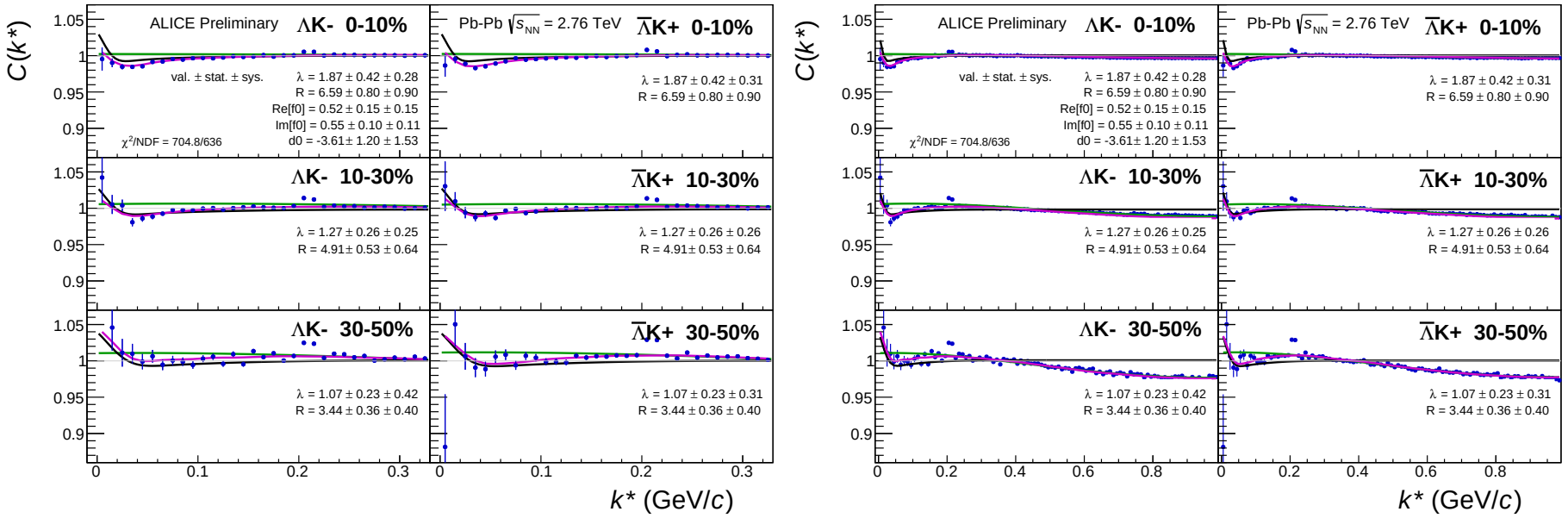

(a) Signal region view ($k^* \lesssim 0.3$ GeV/c)

(b) Wide view ($k^* \lesssim 1.0$ GeV/c)

Fig. 12: Fits, with 10 residual correlations included, to the ΛK^-(left) with $\bar{\Lambda}K^+$ (right) data for the centralities 0-10% (top), 10-30% (middle), and 30-50% (bottom). The lines represent the statistical errors, while the boxes represent the systematic errors. All $\Lambda K^{\pm}$ analyses are fit simultaneously across all centralities (0-10%, 10-30%, 30-50%). Scattering parameters ($\mathbb{R}f_0$, $\mathbb{I}f_0$, d_0) are shared between pair-conjugate systems (i.e. a parameter set describing the ΛK^+ & $\bar{\Lambda}K^-$ system, and a separate set describing the ΛK^- & $\bar{\Lambda}K^+$ system). For each centrality, a radius and λ parameters are shared between all pairs (ΛK^+, $\bar{\Lambda}K^-$, ΛK^-, $\bar{\Lambda}K^+$). Each analysis has a unique normalization parameter. The background is modeled by a (6^{th}-)degree polynomial fit to THERMINATOR simulation. The black solid line represents the primary (ΛK) correlation's contribution to the fit. The green line shows the fit to the non-flat background. The purple points show the fit after all residuals' contributions have been included, and momentum resolution and non-flat background corrections have been applied. The extracted fit values with uncertainties are printed.

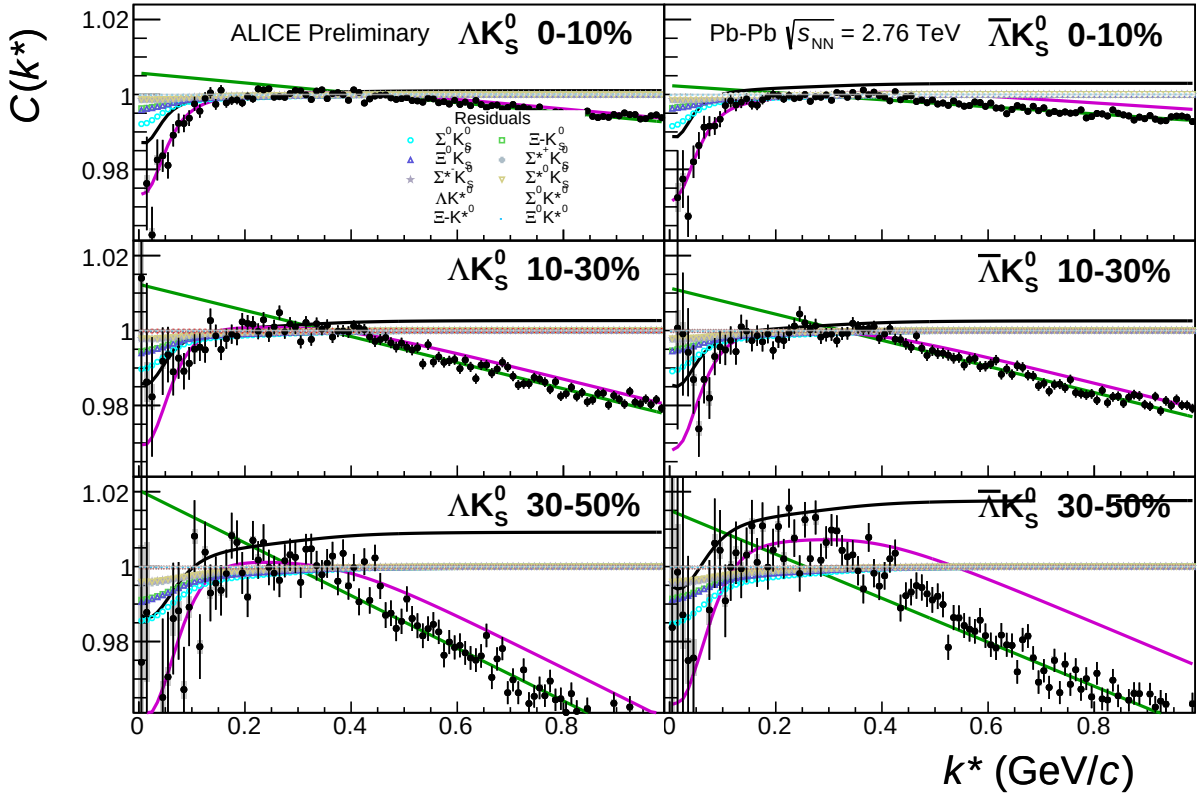

Fig. 13: Fits, with 10 residual correlations included and shown, to the ΛK^0_S (left) and $\bar{\Lambda}K^0_S$ (right) data for the centralities 0-10% (top), 10-30% (middle), and 30-50% (bottom). The ten parent pairs used for the residual correction to the ΛK^0_S ($\bar{\Lambda}K^0_S$) fit are $\Sigma^0K^0_S$, $\Xi^0K^0_S$, $\Xi^-K^0_S$, $\Sigma^{*(+,-,0)}K^0_S$, ΛK^{*0}, Σ^0K^{*0}, Ξ^0K^{*0}, and Ξ^-K^{*0} ($\bar{\Sigma}^0K^0_S$, $\bar{\Xi}^0K^0_S$, $\bar{\Xi}^+K^0_S$, $\bar{\Sigma}^{*(+,-,0)}K^0_S$, $\bar{\Lambda}\bar{K}^{*0}$, $\bar{\Sigma}^0\bar{K}^{*0}$, $\bar{\Xi}^0\bar{K}^{*0}$, and $\bar{\Xi}^+\bar{K}^{*0}$).

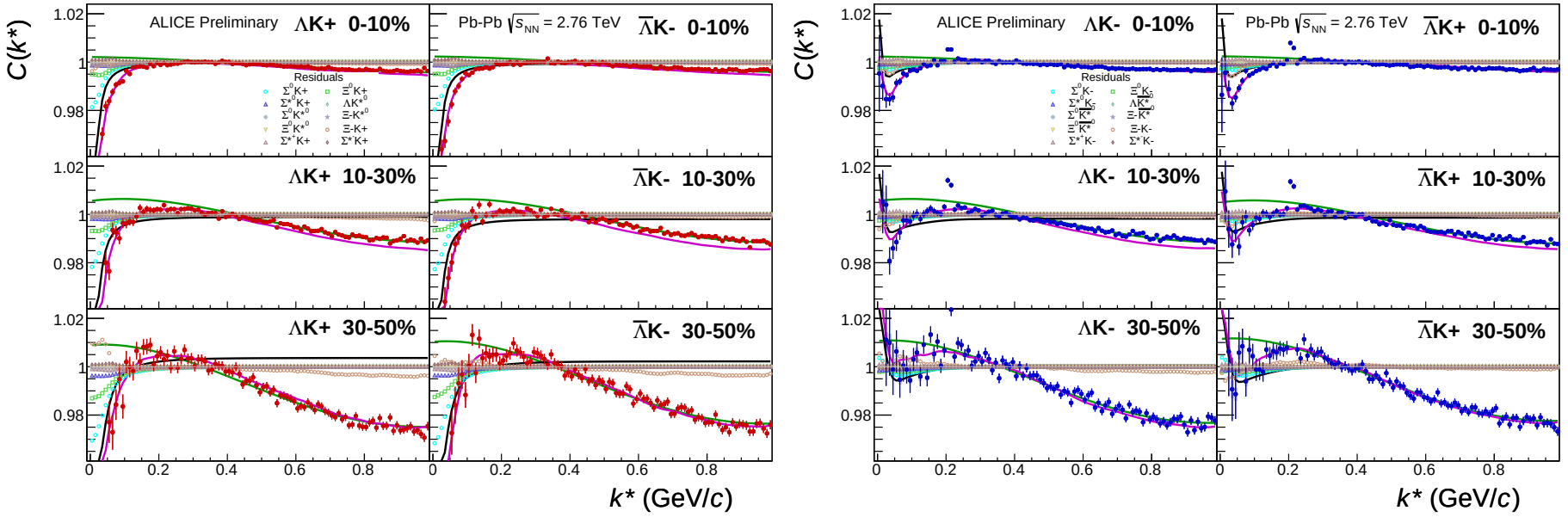

(a) $\Lambda K^+(\bar{\Lambda}K^-)$ fits with residual contributions shown for the centralities 0-10% (top), 10-30% (middle), and 30-50% (bottom)

(b) $\Lambda K^-(\bar{\Lambda}K^+)$ fits with residual contributions shown for the centralities 0-10% (top), 10-30% (middle), and 30-50% (bottom)

Fig. 14: Fits, with 10 residual correlations included and shown, to the ΛK^+ & $\bar{\Lambda}K^-$ (left) and ΛK^- & $\bar{\Lambda}K^+$ (right) data for the centralities 0-10% (top), 10-30% (middle), and 30-50% (bottom). The ten parent pairs used for the residual correction to the ΛK^+ ($\bar{\Lambda}K^-$) fit are Σ^0K^+, Ξ^0K^+, Ξ^-K^+, $\Sigma^{*(+,-,0)}K^+$, ΛK^{*0}, Σ^0K^{*0}, Ξ^0K^{*0}, and Ξ^-K^{*0} ($\bar{\Sigma}^0K^-$, $\bar{\Xi}^0K^-$, $\bar{\Xi}^+K^-$, $\bar{\Sigma}^{*(+,-,0)}K^-$, $\bar{\Lambda}\bar{K}^{*0}$, $\bar{\Sigma}^0\bar{K}^{*0}$, $\bar{\Xi}^0\bar{K}^{*0}$, and $\bar{\Xi}^+\bar{K}^{*0}$).

Fit Results $\Lambda(\bar{\Lambda})K^0_S$

System	Centrality	Fit Parameters				
		λ	R	$\mathbb{R}f_0$	$\mathbb{I}f_0$	d_0
ΛK^0_S & $\bar{\Lambda}K^0_S$	0-10%	0.60 ± 0.71 (stat.) ± 0.54 (sys.)	2.96 ± 0.54 (stat.) ± 0.33 (sys.)	-0.35 ± 0.10 (stat.) ± 0.21 (sys.)	0.19 ± 0.11 (stat.) ± 0.12 (sys.)	1.85 ± 0.61 (stat.) ± 2.68 (sys.)
	10-30%		2.40 ± 0.45 (stat.) ± 0.29 (sys.)			
	30-50%		1.77 ± 0.32 (stat.) ± 0.15 (sys.)			

Table 3: Fit Results $\Lambda(\bar{\Lambda})K^0_S$, with 10 residual correlations included. Each pair is fit simultaneously with its conjugate (ie. ΛK^0_S with $\bar{\Lambda}K^0_S$) across all centralities (0-10%, 10-30%, 30-50%), for a total of 6 simultaneous analyses in the fit. A single λ parameter is shared amongst all. Each analysis has a unique normalization parameter. The radii are shared between analyses of like centrality, as these should have similar source sizes. The scattering parameters ($\mathbb{R}f_0$, $\mathbb{I}f_0$, d_0) are shared amongst all. The background is fit with a linear form in the range $0.6 < k^* < 0.9$ GeV/c. The fit is done on the data with only statistical error bars. The errors marked as "stat." are those returned by MINUIT. The errors marked as "sys." are those which result from my systematic analysis (as outlined in Section **??**).

Fit Results $\Lambda(\bar{\Lambda})K^{\pm}$

System	Centrality	Fit Parameters				
		λ	R	$\mathbb{R}f_0$	$\mathbb{I}f_0$	d_0
ΛK^+ & $\bar{\Lambda}K^-$	0-10%	1.87 ± 0.42 (stat.) ± 0.21 (sys.)	6.59 ± 0.80 (stat.) ± 0.49 (sys.)	-1.14 ± 0.17 (stat.) ± 0.31 (sys.)	0.66 ± 0.16 (stat.) ± 0.15 (sys.)	0.68 ± 0.46 (stat.) ± 0.53 (sys.)
	10-30%	1.27 ± 0.26 (stat.) ± 0.23 (sys.)	4.91 ± 0.53 (stat.) ± 0.28 (sys.)			
ΛK^+ & $\bar{\Lambda}K^-$	30-50%	1.07 ± 0.23 (stat.) ± 0.32 (sys.)	3.44 ± 0.36 (stat.) ± 0.13 (sys.)	0.52 ± 0.15 (stat.) ± 0.19 (sys.)	0.55 ± 0.10 (stat.) ± 0.18 (sys.)	-3.61 ± 1.20 (stat.) ± 1.02 (sys.)

Table 4: Fit Results $\Lambda(\bar{\Lambda})K^{\pm}$, with 10 residual correlations included. All $\Lambda K^{\pm}$ analyses are fit simultaneously across all centralities (0-10%, 10-30%, 30-50%). Scattering parameters ($\mathbb{R}f_0$, $\mathbb{I}f_0$, d_0) are shared between pair-conjugate systems (i.e. a parameter set describing the ΛK^+ & $\bar{\Lambda}K^-$ system, and a separate set describing the ΛK^- & $\bar{\Lambda}K^+$ system). For each centrality, a radius and λ parameters are shared between all pairs (ΛK^+, $\bar{\Lambda}K^-$, ΛK^-, $\bar{\Lambda}K^+$). Each analysis has a unique normalization parameter. The background is modeled by a (6^{th}-)degree polynomial fit to THERMINATOR simulation. The fit is done on the data with only statistical error bars. The errors marked as "stat." are those returned by MINUIT. The errors marked as "sys." are those which result from my systematic analysis (as outlined in Section **??**).

0.1.3 No Residual Correlations Included in Fit

Figure 15 nicely collects and summarizes all of our extracted fit parameters for the case of no included residual contributors. Figure 16 presents our extracted fit radii, along with those of other systems previously analyzed by ALICE [**?**], as a function of pair transverse mass (m_{T}). Figures 17, 18, and 19 show the experimental correlation functions with fits, assuming no residual contributors, for all studied centralities for $\Lambda\mathrm{K}^0_{\mathrm{S}}$ with $\bar{\Lambda}\mathrm{K}^0_{\mathrm{S}}$, $\Lambda\mathrm{K}^+$ with $\bar{\Lambda}\mathrm{K}^-$, and $\Lambda\mathrm{K}^-$ with $\bar{\Lambda}\mathrm{K}^+$, respectively. The parameter sets extracted from the fits can be found in Tables 5 and 6.

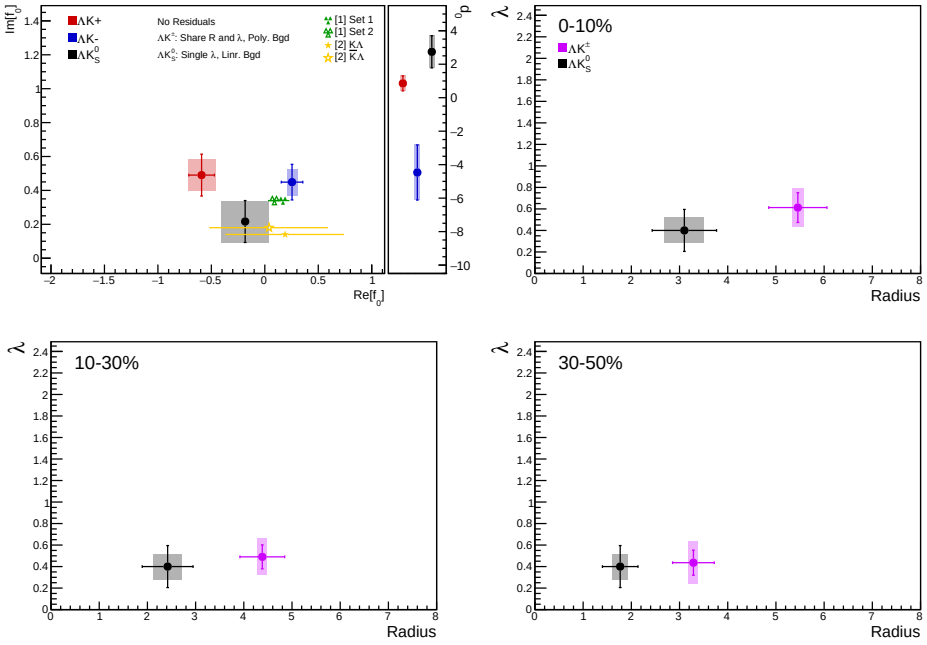

Fig. 15: Extracted scattering parameters for the case of NO residual contributors for all of our ΛK systems. [Top Left]: $\mathbb{I}f_0$ vs. $\mathbb{R}f_0$, together with d_0 to the right. [Top Right (Bottom Left, Bottom Right)]: λ vs. Radius for the 0-10% (10-30%, 30-50%) bin. The green [**?**] and yellow [**?**] points show theoretical predictions made using chiral perturbation theory.

Figure 16 shows extracted R_{inv} parameters as a function of tranverse mass (m_{T}) for various pair systems over several centralities. The published ALICE data [**?**] is shown with transparent, open symbols. The new ΛK results are shown with opaque, filled symbols. The radii shown an increasing size with increasing centrality, as is expected from the simple geometric picture of the collisions. The radii decrease in size with increasing m_{T}, and we see an approximate scaling of the radii with transverse mass, as is expected in the presence of collective flow in the system.

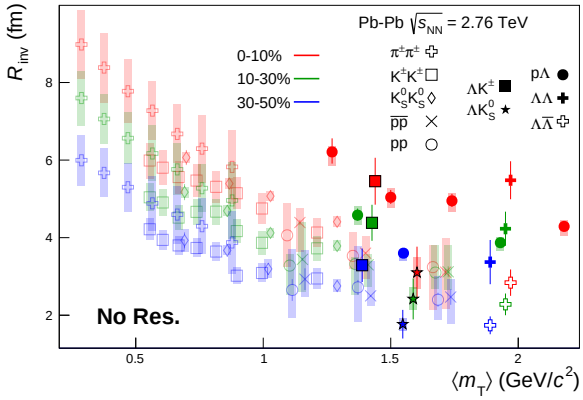

Fig. 16: No residual correlations in ΛK fits. Extracted fit $R_{\rm inv}$ parameters as a function of pair transverse mass ($m_{\rm T}$) for various pair systems over several centralities. The ALICE published data [**?**] is shown with transparent, open symbols. The new ΛK results are shown with opaque, filled symbols. In the left, the ΛK^+ (with it's conjugate pair) results are shown separately from the ΛK^- (with it's conjugate pair) results. In the right, all $\Lambda K^{\pm}$ results are averaged.

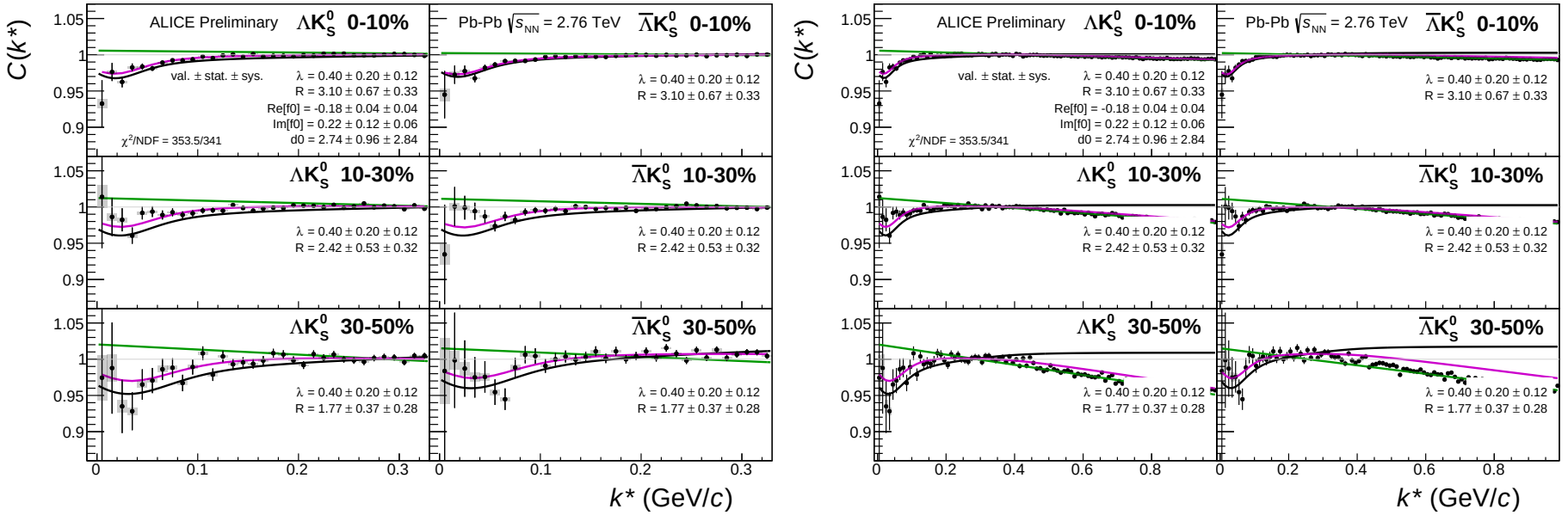

(a) Signal region view ($k^* \lesssim 0.3$ GeV/c)

(b) Wide view ($k^* \lesssim 1.0$ GeV/c)

Fig. 17: Fits, with NO residual correlations included, to the ΛK^0_S (left) and $\bar{\Lambda} K^0_S$ (right) data for the centralities 0-10% (top), 10-30% (middle), and 30-50% (bottom). The lines represent the statistical errors, while the boxes represent the systematic errors. A single λ parameter is shared amongst all. Each analysis has a unique normalization parameter. The radii are shared between analyses of like centrality, as these should have similar source sizes. The scattering parameters ($\mathbb{R}f_0$, $\mathbb{I}f_0$, d_0) are shared amongst all. The background is modeled by a (6^{th}-)degree polynomial fit to THERMINATOR simulation. The black solid line represents the "raw" primary fit, i.e. not corrected for momentum resolution effects nor non-flat background. The green line shows the fit to the non-flat background. The purple points show the fit after momentum resolution and non-flat background corrections have been applied. The extracted fit values with uncertainties are printed.

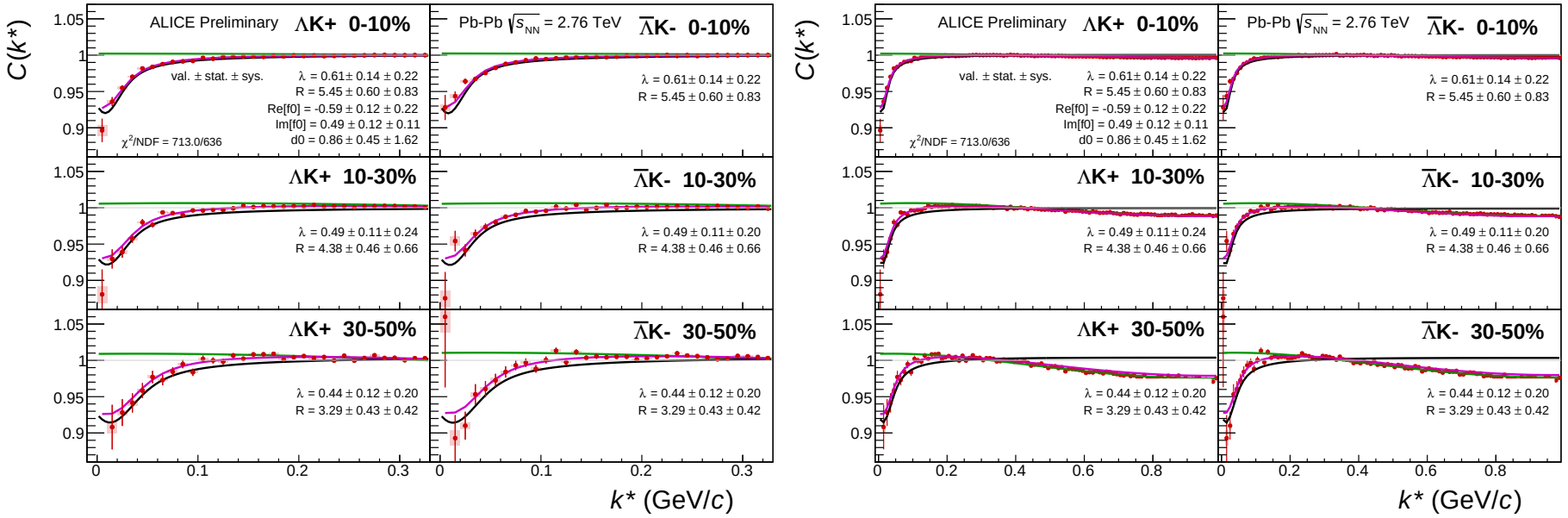

(a) Signal region view ($k^* \lesssim 0.3$ GeV/c)

(b) Wide view ($k^* \lesssim 1.0$ GeV/c)

Fig. 18: Fits to the ΛK^+ (left) and $\bar{\Lambda} K^-$ (right) data for the centralities 0-10% (top), 10-30% (middle), and 30-50% (bottom). The lines represent the statistical errors, while the boxes represent the systematic errors. All $\Lambda K^{\pm}$ analyses are fit simultaneously across all centralities (0-10%, 10-30%, 30-50%). Scattering parameters ($\mathbb{R}f_0$, $\mathbb{I}f_0$, d_0) are shared between pair-conjugate systems (i.e. a parameter set describing the ΛK^+ & $\bar{\Lambda} K^-$ system, and a separate set describing the ΛK^- & $\bar{\Lambda} K^+$ system). For each centrality, a radius and λ parameters are shared between all pairs (ΛK^+, $\bar{\Lambda} K^-$, ΛK^-, $\bar{\Lambda} K^+$). Each analysis has a unique normalization parameter. The background is modeled by a (6^{th}-)degree polynomial fit to THERMINATOR simulation. The black solid line represents the "raw" primary fit, i.e. not corrected for momentum resolution effects nor non-flat background. The green line shows the fit to the non-flat background. The purple points show the fit after momentum resolution and non-flat background corrections have been applied. The extracted fit values with uncertainties are printed.

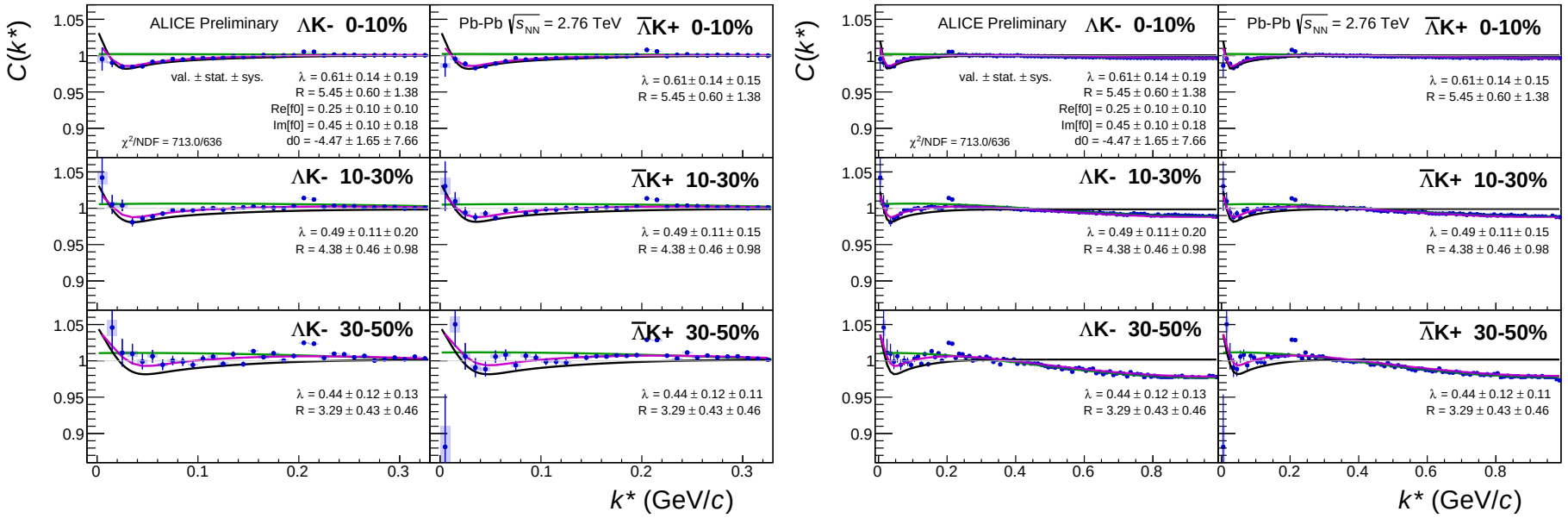

(a) Signal region view ($k^* \lesssim 0.3$ GeV/c)

(b) Wide view ($k^* \lesssim 1.0$ GeV/c)

Fig. 19: Fits, with NO residual correlations included, to the ΛK^-(left) with $\bar{\Lambda}K^+$ (right) data for the centralities 0-10% (top), 10-30% (middle), and 30-50% (bottom). The lines represent the statistical errors, while the boxes represent the systematic errors. All $\Lambda K^{\pm}$ analyses are fit simultaneously across all centralities (0-10%, 10-30%, 30-50%). Scattering parameters ($\mathbb{R}f_0$, $\mathbb{I}f_0$, d_0) are shared between pair-conjugate systems (i.e. a parameter set describing the ΛK^+ & $\bar{\Lambda}K^-$ system, and a separate set describing the ΛK^- & $\bar{\Lambda}K^+$ system). For each centrality, a radius and λ parameters are shared between all pairs (ΛK^+, $\bar{\Lambda}K^-$, ΛK^-, $\bar{\Lambda}K^+$). Each analysis has a unique normalization parameter. The background is modeled by a (6^{th}-)degree polynomial fit to THERMINATOR simulation. The black solid line represents the "raw" primary fit, i.e. not corrected for momentum resolution effects nor non-flat background. The green line shows the fit to the non-flat background. The purple points show the fit after momentum resolution and non-flat background corrections have been applied. The extracted fit values with uncertainties are printed.

Fit Results $\Lambda(\bar{\Lambda})K^0_S$

System	Centrality	Fit Parameters				
		λ	R	$\mathbb{R}f_0$	$\mathbb{I}f_0$	d_0
ΛK^0_S & $\bar{\Lambda}K^0_S$	0-10%	0.40 ± 0.20 (stat.) ± 0.12 (sys.)	3.10 ± 0.67 (stat.) ± 0.41 (sys.)	-0.18 ± 0.04 (stat.) ± 0.22 (sys.)	0.22 ± 0.12 (stat.) ± 0.12 (sys.)	2.74 ± 0.96 (stat.) ± 1.28 (sys.)
	10-30%		2.42 ± 0.53 (stat.) ± 0.29 (sys.)			
	30-50%		1.77 ± 0.37 (stat.) ± 0.16 (sys.)			

Table 5: Fit Results $\Lambda(\bar{\Lambda})K^0_S$, with no residual correlations included. Each pair is fit simultaneously with its conjugate (ie. ΛK^0_S with $\bar{\Lambda}K^0_S$) across all centralities (0-10%, 10-30%, 30-50%), for a total of 6 simultaneous analyses in the fit. A single λ parameter is shared amongst all. Each analysis has a unique normalization parameter. The radii are shared between analyses of like centrality, as these should have similar source sizes. The scattering parameters ($\mathbb{R}f_0$, $\mathbb{I}f_0$, d_0) are shared amongst all. The background is fit with a linear form in the range $0.6 < k^* < 0.9$ GeV/c. The fit is done on the data with only statistical error bars. The errors marked as "stat." are those returned by MINUIT. The errors marked as "sys." are those which result from my systematic analysis (as outlined in Section **??**).

Fit Results $\Lambda(\bar{\Lambda})K^{\pm}$

System	Centrality	Fit Parameters				
		λ	R	$\mathbb{R}f_0$	$\mathbb{I}f_0$	d_0
ΛK^+ & $\bar{\Lambda}K^-$	0-10%	0.61 ± 0.14 (stat.) ± 0.18 (sys.)	5.45 ± 0.60 (stat.) ± 0.12 (sys.)	-0.59 ± 0.12 (stat.) ± 0.13 (sys.)	0.49 ± 0.12 (stat.) ± 0.09 (sys.)	0.86 ± 0.45 (stat.) ± 1.63 (sys.)
	10-30%	0.49 ± 0.11 (stat.) ± 0.17 (sys.)	4.38 ± 0.46 (stat.) ± 0.10 (sys.)			
ΛK^+ & $\bar{\Lambda}K^-$	30-50%	0.44 ± 0.12 (stat.) ± 0.20 (sys.)	3.29 ± 0.43 (stat.) ± 0.10 (sys.)	0.25 ± 0.10 (stat.) ± 0.05 (sys.)	0.45 ± 0.10 (stat.) ± 0.08 (sys.)	-4.47 ± 1.65 (stat.) ± 1.60 (sys.)

Table 6: Fit Results $\Lambda(\bar{\Lambda})K^{\pm}$, with no residual correlations included. All $\Lambda K^{\pm}$ analyses are fit simultaneously across all centralities (0-10%, 10-30%, 30-50%). Scattering parameters ($\mathbb{R}f_0$, $\mathbb{I}f_0$, d_0) are shared between pair-conjugate systems (i.e. a parameter set describing the ΛK^+ & $\bar{\Lambda}K^-$ system, and a separate set describing the ΛK^- & $\bar{\Lambda}K^+$ system). For each centrality, a radius and λ parameters are shared between all pairs (ΛK^+, $\bar{\Lambda}K^-$, ΛK^-, $\bar{\Lambda}K^+$). Each analysis has a unique normalization parameter. The background is modeled by a (6^{th}-)degree polynomial fit to THERMINATOR simulation. The fit is done on the data with only statistical error bars. The errors marked as "stat." are those returned by MINUIT. The errors marked as "sys." are those which result from my systematic analysis (as outlined in Section **??**).

0.1.4 Fit Method Comparisons

In Figure 20, we show extracted fit parameters for the case of $\Lambda K^+(\bar{\Lambda}K^-)$ sharing radii with $\Lambda K^-(\bar{\Lambda}K^+)$. The figure shows results for three different treatments of the non-femtoscopic background: a polynomial fit to THERMINATOR 2 simulation to model the background (circles), a linear fit to the data to model the background (squares), and the Stavinsky method (crosses).

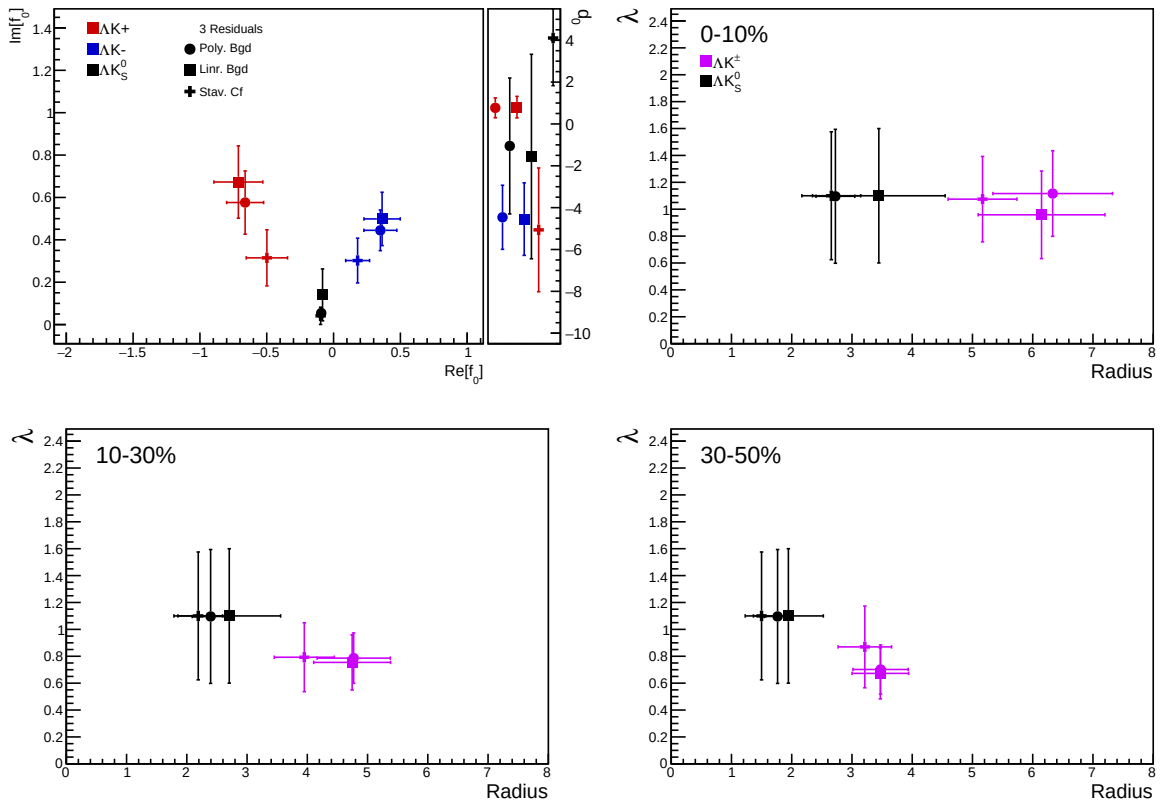

Fig. 20: Compare Fit Parameters: Background treatment: Extracted fit results for all of our $\Lambda(\bar{\Lambda})K^{\pm}$ systems across all studied centrality bins (0-10%, 10-30%, 30-50%). The $\Lambda K^+(\bar{\Lambda}K^-)$ and $\Lambda K^-(\bar{\Lambda}K^+)$ systems share both a radius and a λ parameter for each centrality bin (i.e. 3 total radius parameters, 3 total λ parameters). The figure shows results for three different treatments of the non-femtoscopic background: a polynomial fit to THERMINATOR 2 simulation to model the background (circles), a linear fit to the data to model the background (squares), and the Stavinsky method (crosses). The green [**?**] and yellow [**?**] points show theoretical predictions made using chiral perturbation theory.

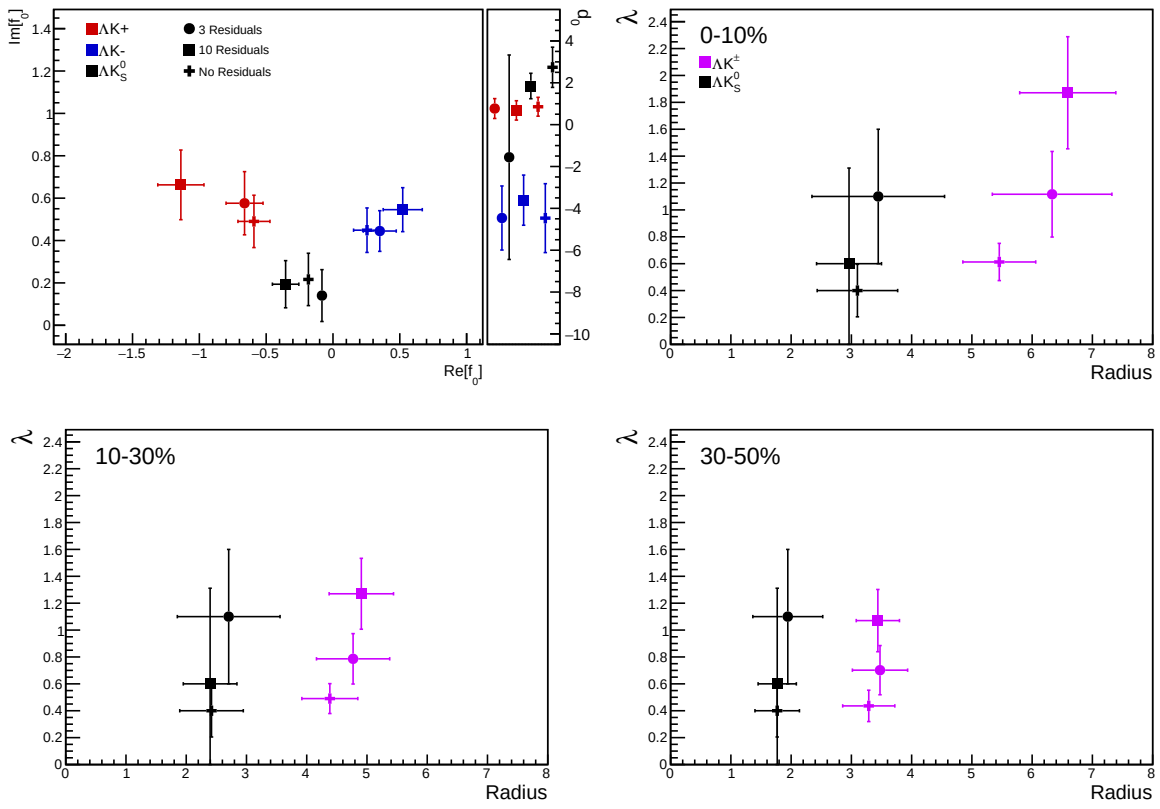

Fig. 21: Compare Fit Parameters: Number of residuals: Results shown for the case of 3 (+), 10 (X), and no (circles) residual contributors.

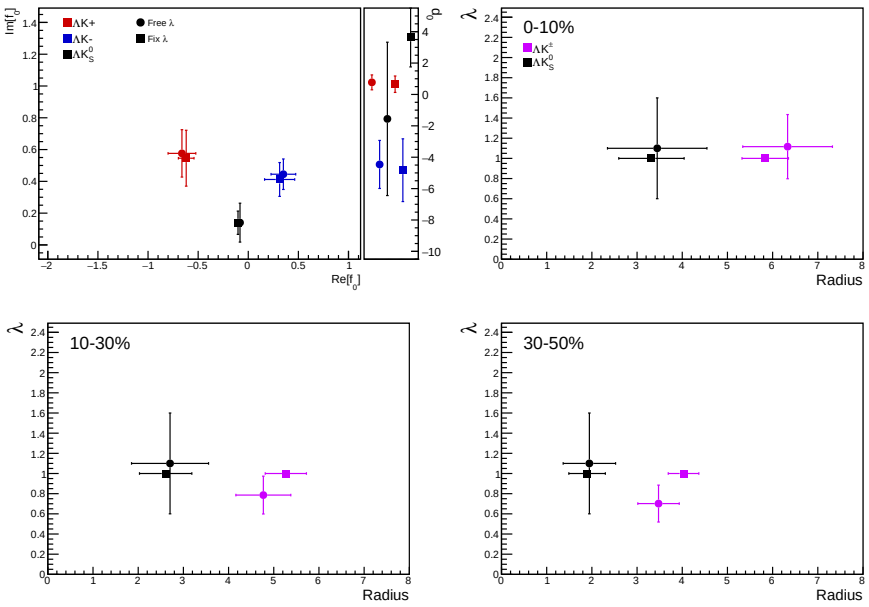

(a) Shared radii

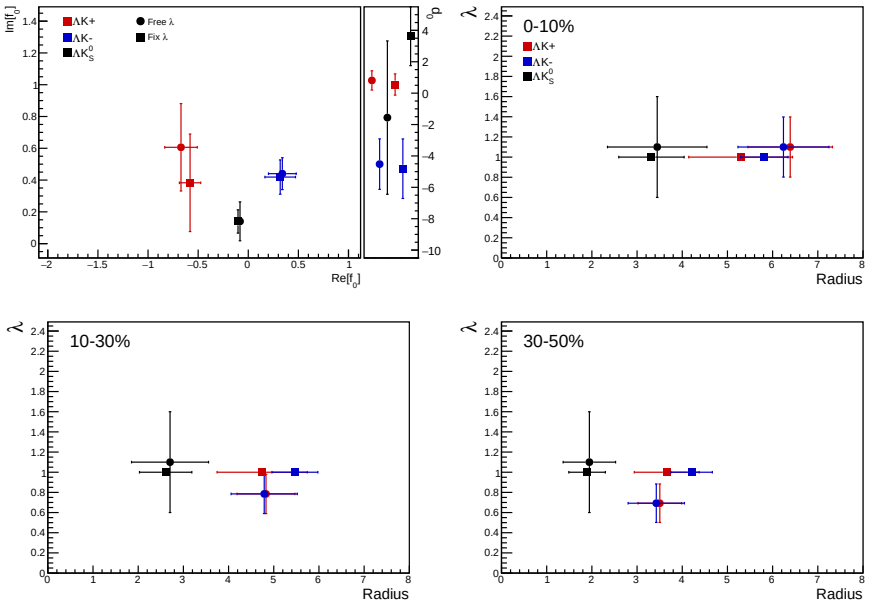

(b) Separate radii

Fig. 22: Compare Fit Parameters: Free vs fixed λ: Results shown for λ parameters left free (filled symbols) and fixed to 1 (open symbols). In the top plot (22a), the ΛK^+ and ΛK^- analyses share radii, whereas in the bottom (22b) they have unique radii.

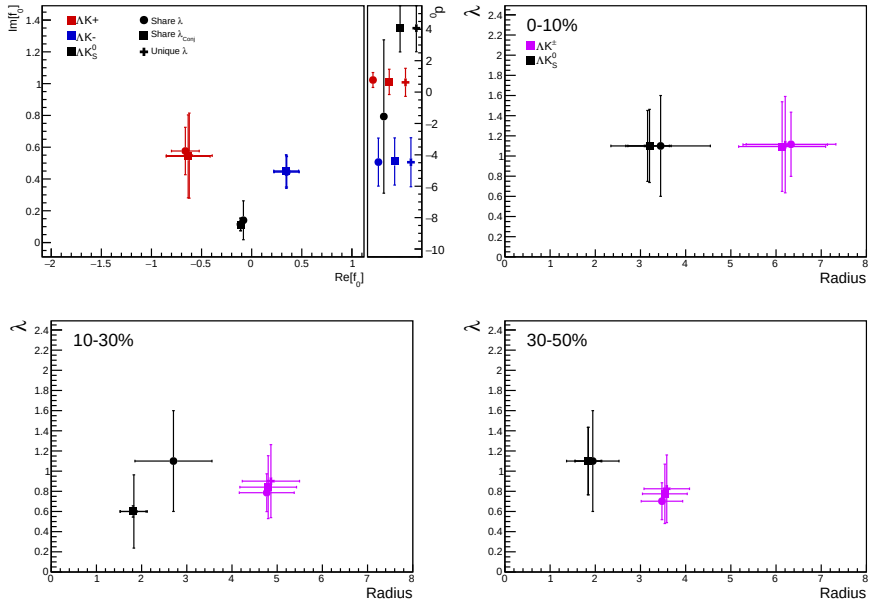

(a) Shared radii

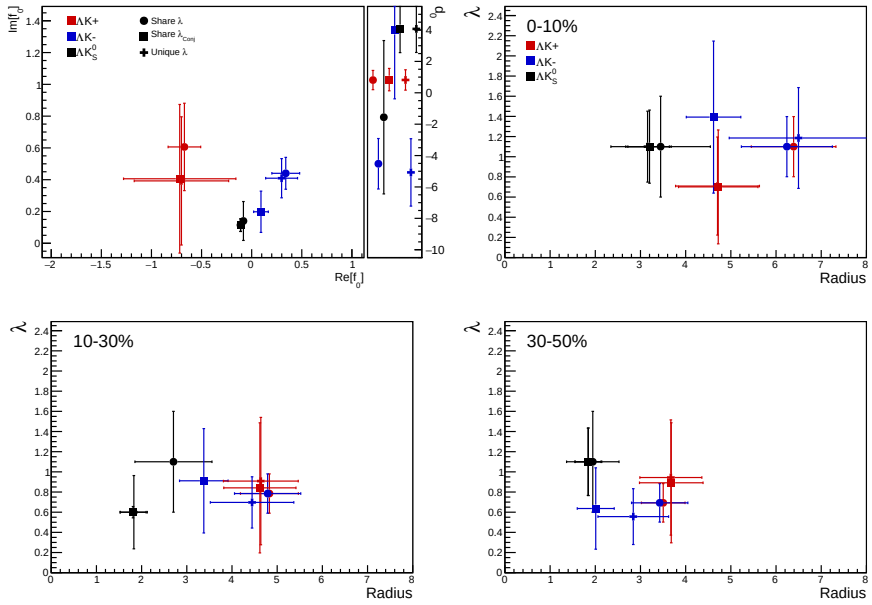

(b) Separate radii

Fig. 23: Compare Fit Parameters: Shared vs unique λ: Results shown for different sharing of the λ parameters between analyses and systems. In the top (23a), the ΛK^+ and ΛK^- analyses share radii, whereas in the bottom (23b), they do not. "Share λ" (circles) is the case where a single λ is shared amongst all analyses for a given centrality bin (i.e., in 23a, 3 radius parameters and 3 λ parameters). "Share λ_{Conj}" (squares) means that conjugate pairs (ex. ΛK^+ and $\bar{\Lambda} K^-$) share a λ parameter for each centrality. This corresponds to 6 total λ parameters (for each of the 3 centrality bins, the $\Lambda K^+(\bar{\Lambda} K^-)$ receives a unique λ, as does $\Lambda K^-(\bar{\Lambda} K^+)$). Finally, in "Unique λ" (+), each analysis received its own unique λ parameter. This corresponds to 12 λ parameters (for each of the 3 centrality bins, each ΛK^+, $\bar{\Lambda} K^-$, ΛK^-, and $\bar{\Lambda} K^+$ receives a unique λ).

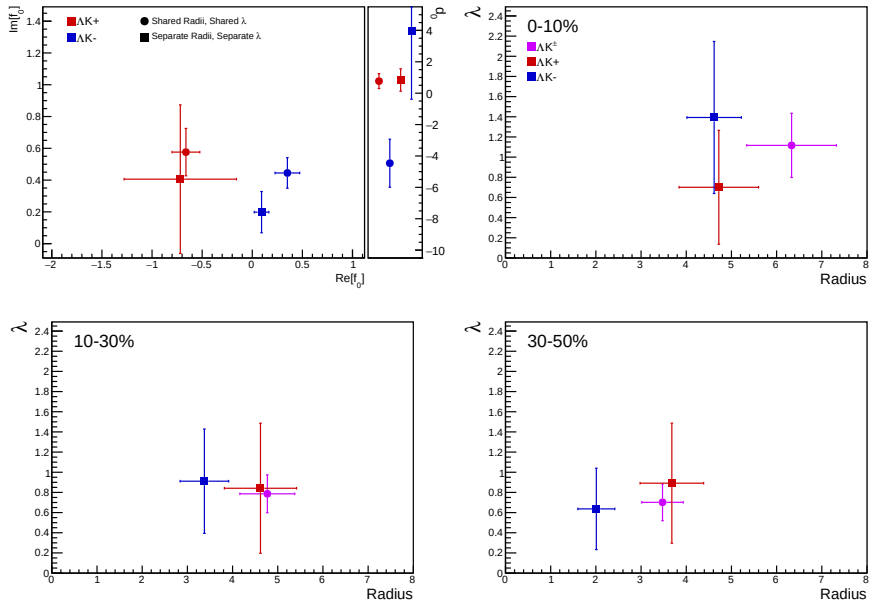

(a) Shared radii

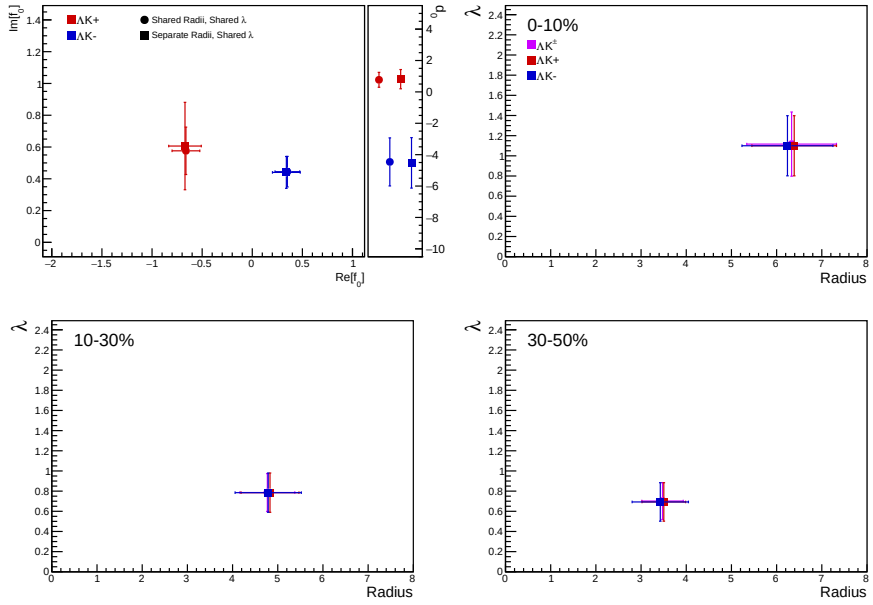

(b) Separate radii

Fig. 24: Compare Fit Parameters: Shared vs. Separate Radii: Results shown for the case of radii being shared between ΛK^+ and ΛK^- (circles) vs not shared (squares). In (a), when the radii are not shared between ΛK^+ and ΛK^-, neither are the λ parameters. In (b), the λ parameters are always shared between ΛK^+ and ΛK^-

0.1.5 *Discussion of m_T-Scaling*

It is clear from the results presented in the previous sections, that the ΛK systems do not conform to the approximate m_T-scaling of the pair source sizes. At first thought, this may appear to be a troubling result; the approximate scaling is an observed consequence of the collective behavior of the soft (low-p_T) sector of the produced system. The Λ and K particles certainly participate in the collective expansion of the QGP medium, so why do their extracted femtoscopic radii not behave as expected? To get straight to the point: the ΛK systems are (obviously) comprised on non-identical particles, each with its own and unique single particle source. Each source is, in general, unique in both its overall size, and in its space-time position within the produced medium. The hydrodynamic nature of the medium produces the approximate m_T-scaling with respect to these single-particle sources, not the pair sources. The combination of these effects, when probing correlations between non-identical particle pairs, leads to extracted radii falling outside of the (identical particle femtoscopy) m_T-scaling trend. Figure 25 (which contains the same data as Fig.2), shows again the R_{inv} vs m_T plot, but also highlights (with arrows) the approximate individual $\langle m_T \rangle$ values of the single particle distributions. The grey circles show how to single particle sizes change with m_T.

Taking a close look at Fig. 25, one can see that the previously published data (transparent points) are for identical particle analyses only. For these cases, the pair source, probed through femtoscopy, is comprised of two identical sources laying on top of each other. The extracted femtoscopic radii are related to the single particle source sizes by a factor of $\sqrt{2}$, and of course follow the m_T-scaling trend. The other (unpublished) non-identical particle femtoscopic study (pΛ) included in the figure, also shows radii deviating from the m_T-scaling band. Drawing a comparison with the ΛΛ̄ study shown in Fig. 2 is a bit more complicated; the ΛΛ̄ system, although containing non-identical particles, does contain a particle with its antiparticle, for which annihilation could conceivably alter the pair source distribution. It would be more surprising if the non-identical analyses did happen to conform to the scaling; although, this could occur for a non-identical analysis in which the particles have similar masses as well as similar m_T distributions. For the case presented here, the result differing from m_T-scaling is not surprising.

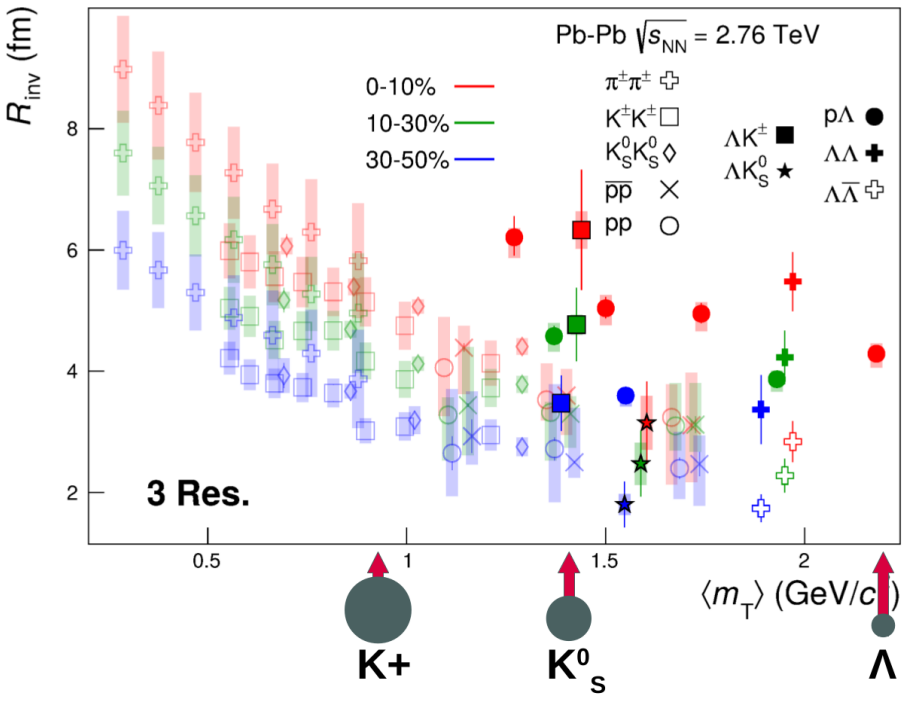

Fig. 25: Same as Fig. 2, but with the individual m_T values for the single particle distributions identified. The grey circles show how the single particle sizes are expected to change with m_T.

I will also briefly point out that it is not automatically clear where a non-identical study should be placed on such a $R_{\rm inv}$ vs $m_{\rm T}$ plot. Each single particle distribution has a well-defined $\langle m_{\rm T} \rangle$, which, to a large extent, determines the single particle region of homogeneity. When combining two sources with different spatio-temporal characteristics, originating from particles of different $m_{\rm T}$, how should one define the pair $m_{\rm T}$? A simple mathematical expression for the pair $m_{\rm T}$ is easy to come up with, but that's not exactly what I'm hinting at here. With respect to this $m_{\rm T}$-scaling picture, the $m_{\rm T}$ value dictates the source size, and one desires the same for non-identical particles. However, do the two unequal sized sources both contribute equally to the extracted femtoscopic size? Or does the larger (smaller) source more closely dictate the femtoscopic signal? If the contribution is equal, then it seems natural to simply more-or-less average the two, single particle, $m_{\rm T}$ values. If the contribution is unequal, then there should be introduced some sore of weighting in the pair $m_{\rm T}$ calculation reflecting this fact. In any case, in our study we use the most straightforward definition of pair $m_{\rm T}$, defined as:

$$m^2_{\rm T,pair} = \left(\frac{m_{\rm inv}}{2}\right)^2 + \left(\frac{1}{2}|\boldsymbol{p}_{\rm T,1} + \boldsymbol{p}_{\rm T,2}|\right)^2 \tag{1}$$

Many times, the equation for non-identical particle pair $m_{\rm T}$ is defined with the average mass replacing $m_{\rm inv}/2$. However, the above Eq. 1 is more directly analogous to the single particle $m_{\rm T}$:

$$m^2_{\rm T} = m^2 + \boldsymbol{p}^2_{\rm T} = (p^0)^2 - (p^3)^2 \tag{2}$$

as, Eq. 1 may be rewritten as:

$$\begin{aligned} m^2_{\rm T,pair} &= (K^0)^2 - (K^3)^2 \\ K^\mu &\equiv \frac{1}{2}\left(p^\mu_1 + p^\mu_2\right) \end{aligned} \tag{3}$$

Identical particle femtoscopic studies are able to probe only the size of the emitting region, or, more precisely, the second moments of the emission function. In addition to this, non-identical particle studies are able to measure the relative emission shifts, the first moments of the emission function. One method to extract information about the emission asymmetries in the system is via a spherical decomposition of the correlation function. With this method, one can draw a wealth of information from just a few components of the decomposition. More specifically, the C_{00} component is similar to the 1D correlation functions typically studied, and probes the overall size of the source. The $\Im C_{11}$ component probes the asymmetry in the system; a non-zero value reveals the asymmetry.

In Fig. 26 we show results for the C_{00} and $\Im C_{11}$ components from the spherical decomposition of our ΛK^+ system in the 0-10% centrality bin (red circles). Results from a number of other components within the decomposition, as well as for our ΛK^0_S and ΛK^- systems, are contained in **??**. Along with the experimental data in Fig. 26, we have also included results from THERMINATOR simulation for an impact parameter of b = 2 fm (gold stars). As THERMINATOR does not include any final state effects, we assumed scattering parameters ($\Re f_0, \Im f_0, d_0$) = (-1.16, 0.51, 1.08) and weighted the numerator pairs with $|\Psi|^2$, as discussed previously. As seen in the figure, the C_{00} signal is similar to that observed in our one-dimensional study. The $\Im C_{11}$ component shows a clear deviation from zero, and the negative value signifies that the Λ particles are, on average, emitted further out and/or earlier than the K mesons.

Fig. 27 shows a closer look at the THERMINATOR simulation, whose spherical harmonic decomposition was shown along with the data in Fig. 26. The top left of Fig. 27a shows a fit to the one-dimensional correlation function from THERMINATOR. The scattering parameters are known precisely here, as they served as the weights used in the simulation, and are kept constant in the fit. We are interested at looking

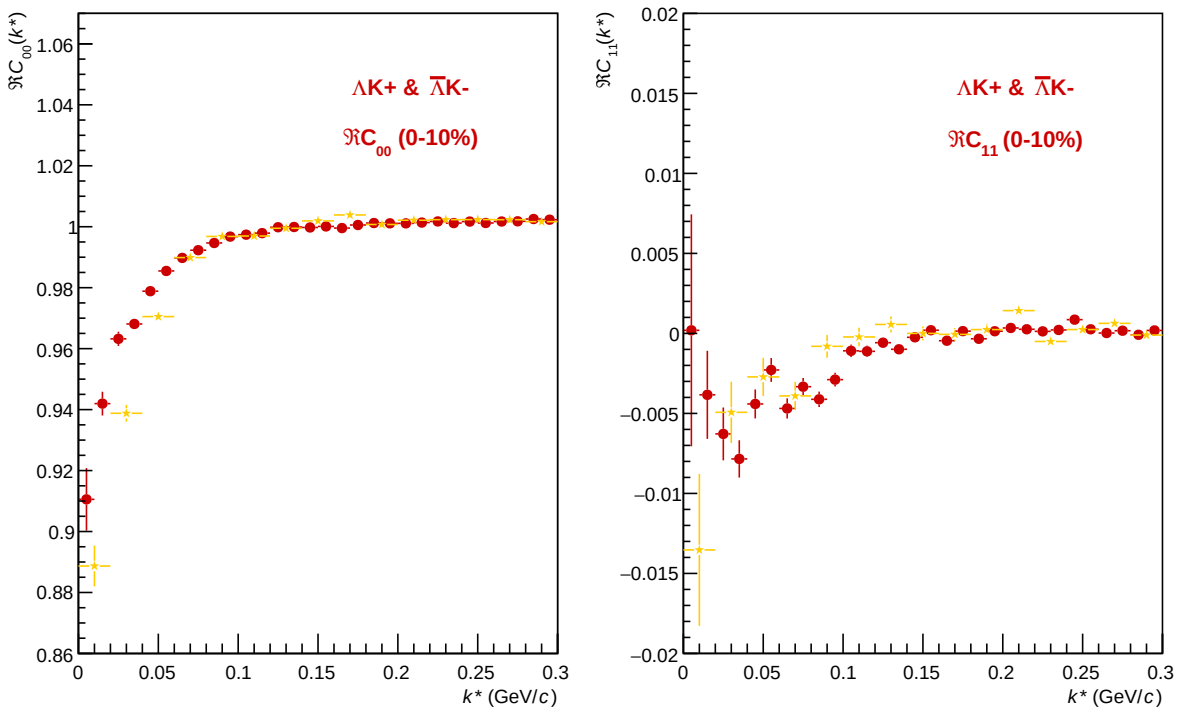

Fig. 26: C_{00} (left) and $\Im C_{11}$ (right) components of a spherical harmonic decomposition of the ΛK^+ correlation function for the 0-10% centrality bin. The C_{00} component is similar to the 1D correlation functions typically studied, and probes the overall size of the source. The $\Im C_{11}$ component probes the asymmetry in the system; a non-zero value reveals the asymmetry

at the extracted one-dimensional source size here, so the λ parameter is also fixed at unity. The other three plots in Fig. 27a show the source distribution in the out (top right), side (bottom left), and long (bottom right) directions (all in the PRF). The source distributions have all been fitted with a Gaussian form, the result of which is printed within the respective plot. One immediately sees a significant shift in the out direction, $\mu_{\text{out}} \approx 4$ fm, and negligible shift in the other two directions, $\mu_{\text{side}} \approx \mu_{\text{long}} \approx 0$ fm. The figure demonstrates that, within the THERMINATOR model, the Λ is, on average, emitted further out that its K partner. Finally, Fig. 27b shows the distribution of the relative time of emittance, again in the PRF. The figure shows that the Λ is, on average, emitted earlier than its K partner.

We end this section with a brief look at how a spatial separation of the single particle sources affects the radii extracted from a femtoscopic analysis. To achieve this, we use THERMINATOR in a similar fashion as described above, but with one important difference. Instead of taking the source information from THERMINATOR, we instead draw the source from a pre-determined Gaussian distribution. In all cases, we take $R_{\text{out}} = R_{\text{side}} = R_{\text{long}} = 5$ fm, and $\mu_{\text{side}} = \mu_{\text{long}} = 0$ fm. Figure 28 shows an example of results obtained from THERMINATOR following this procedure, where $\mu_{\text{out}} = 3$ fm.

In Figure 29, we show results for the case of $\mu_{out} = 1$ fm, $\mu_{out} = 3$ fm, and $\mu_{out} = 6$ fm. In this figure, we do not show the side and long distributions, as they appear identical to those shown in Fig. 28. The figure demonstrates that as the separation μ_{out} increases, so do the extracted femtoscopic radii.

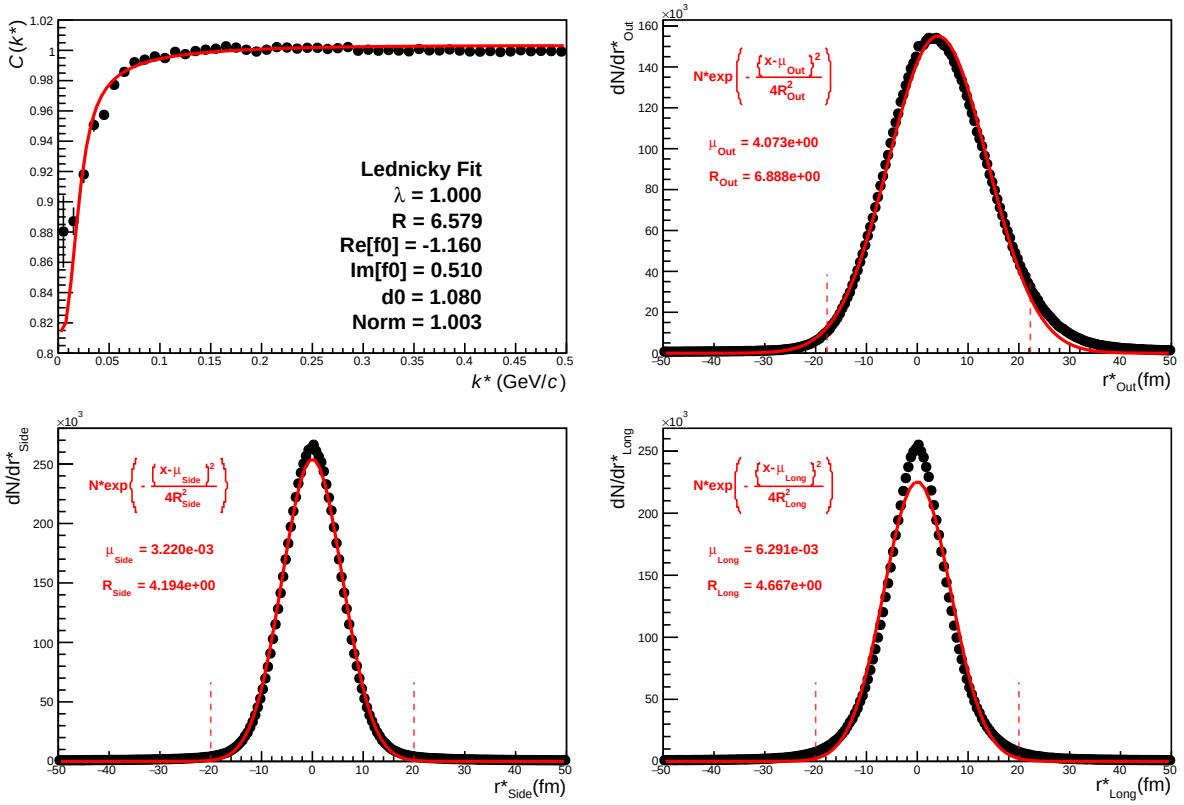

(a) Caption 1

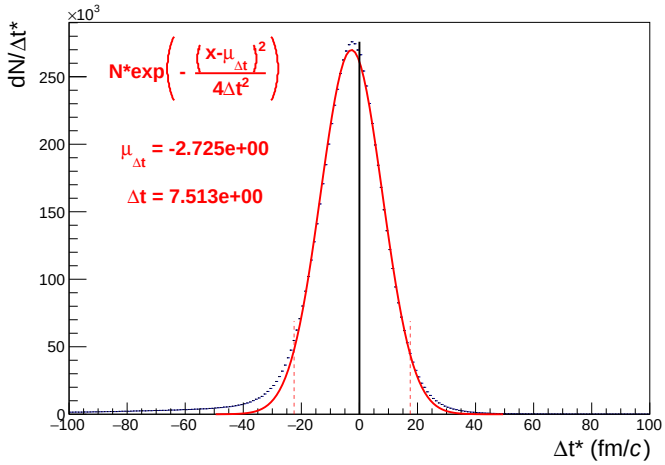

(b) Caption 2

Fig. 27: Long Overall

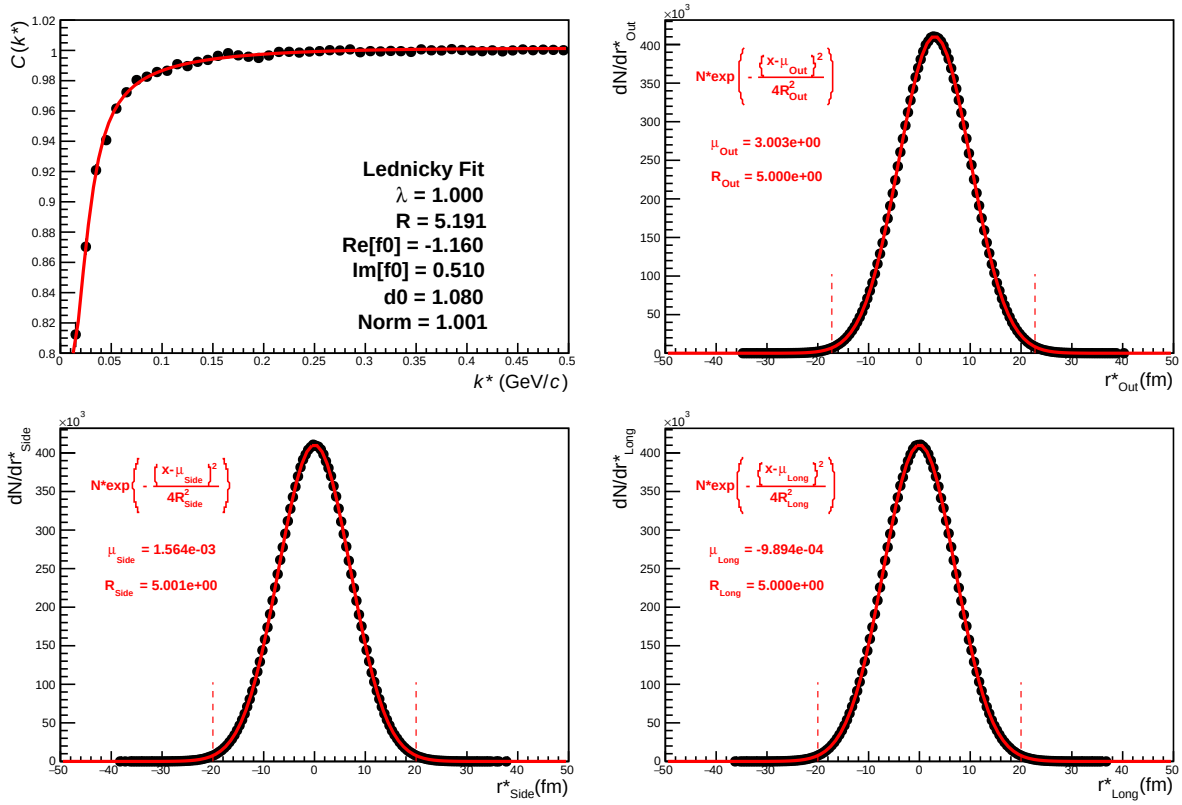

Fig. 28: Long Caption

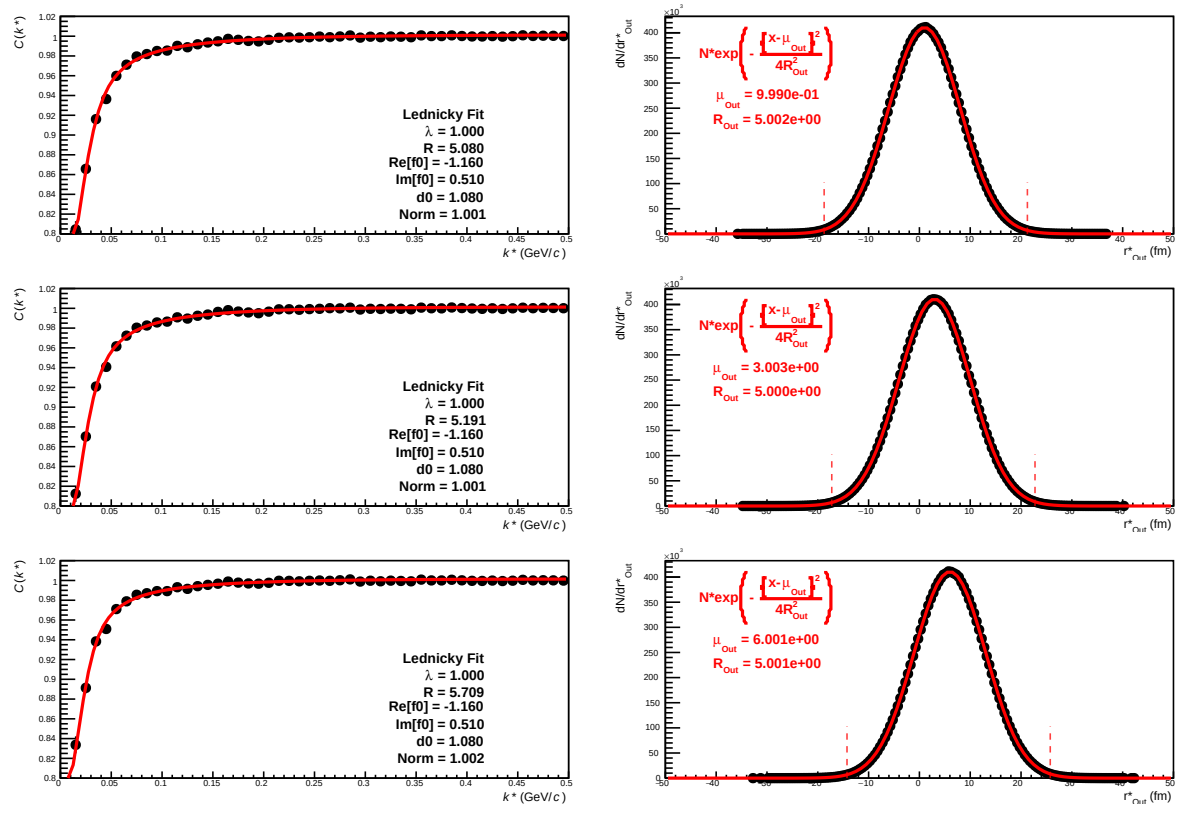

Fig. 29: Long Caption